Environmental Science
Processes & Impacts

Use of Sequential Extraction and Mercury Stable Isotope Analysis to Assess Remobilization of Sediment-Bound Legacy Mercury

Journal:	*Environmental Science: Processes & Impacts*
Manuscript ID	EM-ART-01-2021-000019.R1
Article Type:	Paper

Environmental Significance Statement

Anthropogenic releases of mercury, a toxic heavy metal, can persist in sediment and soil for decades or longer. Although mercury minerals are largely resistant to dissolution, recent evidence suggests that recalcitrant legacy mercury may represent a long-term source of dissolved mercury to waterbodies. However, it is difficult to identify the specific processes and mechanisms involved in this remobilization. Our study provides a framework for using sequential extractions and mercury isotope analysis to investigate the remobilization of legacy mercury within freshwater ecosystems. These methods allow us to assess which biogeochemical reactions may be occurring within the environment that influence the chemical forms of mercury, which in turn influence its mobility and bioavailability.

Use of Sequential Extraction and Mercury Stable Isotope Analysis to Assess Remobilization of Sediment-Bound Legacy Mercury

Elizabeth R. Crowther,*[a] Jason D. Demers,[a] Joel D. Blum,[a]
Scott C. Brooks,[b] Marcus W. Johnson[a]

[a]Department of Earth and Environmental Sciences, University of Michigan,
1100 N. University Ave., Ann Arbor, MI 48109-1005, USA.

[b]Environmental Science Division, Oak Ridge National Laboratory,
P.O Box 2008, Oak Ridge, TN 37831-6038, USA.

*Corresponding author: Elizabeth R. Crowther, email: ecrowth@umich.edu

ABSTRACT

The goal of this project was to assess how anthropogenic legacy mercury (Hg) retained in streambed sediment may be remobilized to stream water. To do this, we performed sequential extractions and Hg isotope analyses on streambed sediment collected along the length of East Fork Poplar Creek, a point-source contaminated stream in Oak Ridge, Tennessee, USA. Legacy Hg within streambed sediment appears to have been isotopically fractionated by equilibrium isotope effects driven by isotope exchange between co-existing Hg(0) and Hg(II) species, probably over-printing fractionation patterns that would have been imparted by kinetic redox reactions. Weakly-bound and recalcitrant sediment Hg pools were isotopically similar to one another, suggesting that small amounts of recalcitrant Hg may be released and then rapidly and weakly re-adsorbed onto the sediment. This weakly-bound Hg pool appears to contribute dissolved Hg to the hyporheic pore water, which may subsequently enter the surface flow. The isotopic composition of the organically-bound sediment Hg pools, as well as biofilm and suspended particulates, converged with that of the weakly-bound and recalcitrant sediment Hg pools along the flow path. This appears to be indicative of both physical mixing with streambed sediment and the transfer of weakly-bound sediment Hg into biofilm and suspended particulates followed by re-incorporation into the organically-bound sediment Hg pool. Overall, these results provide evidence that legacy Hg in the streambed is remobilized, enters the stream water as dissolved Hg, and may be incorporated into streambed biofilm, which constitutes a basal resource within the stream ecosystem.

1. INTRODUCTION

Mercury (Hg) is a toxic metal that is harmful to the health of humans and wildlife.[1,2] Anthropogenic Hg has been emitted to the atmosphere through fossil fuel combustion, cement and metals production, waste incineration, and artisanal small-scale gold mining, or released directly to waterbodies during mercury and gold mining activities, chlor-alkali production, and other industrial processes.[3] In point-source contaminated aquatic ecosystems, direct industrial releases of Hg can persist in sediment and soil for decades or longer.[4] Although this legacy Hg primarily exists in recalcitrant forms (resistant to dissolution and mobilization), recent evidence suggests that some legacy Hg pools may be remobilized to surface water or become bioavailable for methylation and subsequent accumulation in the food web.[5-8] In order to understand the long-term effects of legacy Hg on water quality and bioaccumulation, it is necessary to assess whether dissolved Hg in contaminated aquatic ecosystems can be derived from seemingly recalcitrant legacy sources in the sediment and soil. Quantifying the legacy Hg pools that may be available for remobilization, as well as the processes governing their release, is essential for predicting the timing and potential for recovery of aquatic ecosystems heavily contaminated with point-source Hg pollution.

In the 1950s and early 1960s, the Y-12 National Security Complex (Y-12) in Oak Ridge, Tennessee used approximately 11 million kg of liquid elemental mercury (Hg(0)) for lithium-6 isotope separation for use in nuclear weapons. During that time, ~193,000 kg of metallic Hg(0) was lost to the soil from spills and leaks within the Y-12 boundary,[9,10] and ~128,000 kg of Hg was discharged from Y-12 directly into East Fork Poplar Creek (EFPC), primarily in the form of dissolved and particulate-bound oxidized mercury (Hg(II)).[10] The headwaters of EFPC originate from Y-12 and are comprised of industrial wastewater, storm water runoff, and contaminated groundwater. Although the release of Hg into EFPC has declined dramatically since the 1960s, total Hg flux measured at the Y-12 boundary has continued to fluctuate between 2.7 and 24 kg per year over the last two decades.[11] This has maintained unfiltered stream water total Hg concentrations of 198 to 1860 ng L^{-1} and dissolved Hg concentrations of 45 to 100 ng L^{-1} at the Y-12 boundary.[11,12]

In addition to continued Hg discharge from Y-12, Hg flux measurements in the lower reaches of EFPC indicate that the stream also receives significant amounts of Hg from diffuse legacy sources, such as hyporheic discharge and riparian floodplain inputs. Field studies have

shown that 25 to 83% of the particulate-bound Hg flux and 6 to 36% of the dissolved Hg flux originates from diffuse legacy sources, as measured at a site ~18 km downstream of the Y-12 boundary.[6,13] Although this recent research suggests that a substantial amount of Hg enters the stream from legacy sources, the specific sources (e.g., streambed sediment, stream bank soil, floodplain soil, and hyporheic pore water) and mechanisms of remobilization remain unclear.

Estimates of the current watershed inventories of Hg include 334 kg in the EFPC streambed[14] and 57,000 kg in the floodplains[15] downstream of Y-12. Each year, an estimated 26 to 38 kg of Hg are contributed to the streambed by bank erosion.[15-17] Results of previous sequential extractions show that EFPC soil and sediment contain high proportions of recalcitrant Hg,[14,18] likely in the form of mercuric sulfide (HgS). The presence of metacinnabar, a polymorph of HgS, has been confirmed in EFPC stream bank and floodplain soil using scanning electron microscopy with energy-dispersive x-ray spectrometry, along with transmission electron microscopy with select area electron diffraction.[18,19] While HgS is a poorly soluble form of Hg,[20] chemical dissolution of solid HgS can occur by sulfide replacement with another ligand, by Hg replacement with another metal, or by sulfide ligand oxidation.[21] For example, dissolved organic matter (DOM) with high aromaticity has been shown to enhance dissolution of HgS by replacing the sulfide ligand, forming dissolved Hg-DOM complexes.[22,23] Additionally, Vázquez-Rodríguez *et al.*[24] found evidence of microbially mediated dissolution of HgS occurring within the hyporheic zone of EFPC. Turbulent hydrodynamic conditions or lowering of the water table may also lead to oxidative dissolution of HgS by high levels of dissolved oxygen, resulting in the release of dissolved Hg, as has been studied experimentally under dissolved oxygen concentrations that roughly meet or exceed 100% dissolved oxygen saturation.[25-27] Through these mechanisms, slow dissolution of legacy HgS and other Hg minerals in highly contaminated ecosystems can release a substantial amount of dissolved Hg over time, which is more mobile and reactive and potentially more bioavailable for methylation.

Contaminated sediment and soil often contain numerous forms of Hg with diverse chemical and physical properties, making it difficult to isolate individual Hg compounds. However, several sequential extraction schemes have been developed to isolate operationally-defined pools of Hg (summarized by Issaro *et al.*[28]). Although sequential extractions are limited in their ability to completely separate different forms of Hg, these operationally-defined pools can be used to generalize the potential mobility and bioavailability of Hg in sediment or soil.

Sequential extraction analyses previously performed on EFPC stream bank soil and streambed sediment showed that 0.11 ± 0.06% (1SD, n=22) of the total Hg in bank soil,[17] and 0.18 to 0.30% (interquartile range, n=66) of the total Hg in streambed sediment,[14] was water soluble. Based on estimates of the total amount of Hg in the streambed, this suggests that 0.6 to 1 kg of the Hg in the entire streambed is weakly bound.[6,14] Similarly, annual dissolved Hg flux measurements in the lower reaches of the stream have ranged from 0.53 to 1.00 kg y^{-1}.[13,29] While the results of water leaching experiments may not be directly comparable to dissolved Hg flux estimates in the stream, these values suggest that, despite the recalcitrant nature of the soil- and sediment-bound Hg, these legacy Hg sources could account for a large proportion of the dissolved Hg flux in the surface water.[6,13] However, it is difficult to demonstrate the *in situ* dissolution of legacy Hg source(s) that contribute to the dissolved Hg flux in stream water, as well as to identify the biogeochemical processes influencing this remobilization.

Mercury stable isotope ratio measurements can be used to track Hg cycling through complex ecosystems. As demonstrated by laboratory experiments, Hg isotopes undergo mass-dependent fractionation (MDF) during all known biotic and abiotic chemical reactions, as well as mass-independent fractionation (MIF) during photochemical reactions and some dark abiotic reactions.[30] The magnitude and sign (positive or negative) of MDF and MIF signatures in environmental samples are useful for determining which biogeochemical reactions are likely to have taken place within an ecosystem, and are also useful for distinguishing between different sources of Hg contamination. Previous and ongoing studies have characterized the Hg stable isotopic composition of surface water, hyporheic pore water, shallow riparian groundwater, suspended particulates, biofilm, streambed sediment, and fish collected from EFPC to identify sources of Hg to the sediment and the stream water.[6,31,32] These studies suggest that hyporheic pore water was predominantly responsible for the diffuse legacy input of dissolved Hg to the surface water.[6] However, previous studies were unable to link the isotopic composition of the hyporheic pore water to its specific legacy source(s).

Different pools of Hg within a single legacy source may have unique isotopic signatures, as demonstrated by other studies that have paired leaching experiments with Hg isotope analysis.[33-39] Thus, isolating and analyzing individual Hg pools can aid in the investigation of *in situ* transformation and remobilization of legacy Hg. In this study, we used sequential extraction methods coupled with Hg stable isotope ratio measurements (1) to assess whether certain pools

of legacy Hg within streambed sediment contribute dissolved Hg to the hyporheic pore water and/or surface water of EFPC and (2) to further investigate the biogeochemical processes underlying the net flux of dissolved Hg into the surface water of EFPC from diffuse legacy sources. Our results are interpreted within the context of our previous investigations of Hg stable isotope fractionation patterns in the sediments, surface water, pore water, and biofilm in EFPC.

2. METHODS

2.1 Streambed Sediment Sample Collection

East Fork Poplar Creek is a 26-kilometer-long low order stream in the Valley and Ridge physiographic province of east Tennessee, USA. Streambed sediment was collected from four sites along EFPC under baseflow conditions during late summer 2017. Downstream sampling followed a gradient of decreasing dissolved and suspended particulate-bound total Hg concentrations.[6,40] Sampling sites were identified by their distance in river kilometers upstream of the confluence of Poplar Creek and EFPC. Streambed sediment was collected from EFK 22.3, EFK 18.0, EFK 15.8, and EFK 8.7, where EFK = East Fork and the number indicates creek kilometer. These locations correspond to hyporheic piezometer and groundwater well sites used for past and ongoing Hg studies[6,15,18] (Figure 1).

Polycarbonate core tubes (4.5 cm diameter), cleaned with 10% HCl, were used to collect streambed sediment from depositional zones. Fifteen core samples of the top ~10 cm of sediment were collected at each site and were combined in a new 5-gallon plastic bucket that had been rinsed with stream water prior to use. Using stream water, sediment was wet sieved in the field into four size fractions: 1-2mm, 250µm-1mm, 125-250µm, and <125µm. Sediment samples were placed on ice in the field, frozen the same day upon arrival at the laboratory (within six hours), and were later freeze-dried, transferred to clean borosilicate glass jars, sealed in doubled Ziploc bags, and then stored in the dark at room temperature. The <125µm size fraction was obtained by collecting the stream water that had flowed through the column of sieves into new trace metal clean 1 L HDPE bottles, which were put on ice in the field and frozen upon return to the laboratory the same day. Later, these sample bottles in which sediment had settled were thawed overnight at room temperature and the liquid overlaying the sediment was removed from the bottles using a vacuum pump before re-freezing and freeze drying the settled <125µm sediment fraction. The mass fraction of each grain size is provided in Table S1.

2.2 Bulk Sediment Mercury Extraction by Combustion

Aliquots of streambed sediment collected from EFK 22.3, EFK 18.0, EFK 15.8, and EFK 8.7 were prepared for analysis of total mercury (THg) concentration and Hg stable isotope ratios following a previously-described combustion procedure.[41] Freeze-dried sediment was ground in 2 g aliquots using a SPEX 8000 Mixer/Mill with an alumina grinding cylinder and ball, and stored in trace metal clean borosilicate glass vials prior to combustion. Four additional aliquots, one per size fraction, were ground separately as sample replicates. To avoid cross contamination, Ottawa Sand (quartz, Fisher Scientific) was ground between each sample, and the grinding cylinder and ball were rinsed thoroughly with deionized water and isopropanol. Aliquots of ground sediment (50 to 100 mg) were combusted in a two-stage furnace, and volatilized Hg(0) was trapped in a 24 g oxidizing solution of 1% $KMnO_4$ (w/w) in 10% H_2SO_4 (v/v) (hereafter, 1% $KMnO_4$). For each size fraction, a replicate aliquot of ground sediment from a single vial was combusted separately as an analytical process replicate. Trap solutions of 1% $KMnO_4$ were later reduced with hydroxylamine hydrochloride ($HONH_3Cl$), and a small aliquot was analyzed for THg concentration using cold vapor atomic fluorescence spectrometry (CVAFS; RA-3F, Nippon Instruments) following EPA Method 1631.[42] Samples were analyzed in batches with quality control including calibration verification standards, secondary standards, and blanks (see Section S1 in the Supporting Information for details).

To reduce matrix interferences from combustion residues, aliquots of the 1% $KMnO_4$ combustion trap solutions were reduced with stannous chloride ($SnCl_2$), and Hg(0) was transferred to secondary 1% $KMnO_4$ trap solutions.[41] These secondary solutions were later reduced with $HONH_3Cl$, and a small aliquot was analyzed for THg concentration by CVAFS. This was done to assess the percent recovery of the transfer process and to allow matching of standard and sample concentrations for isotope analysis. Recovery of Hg after the transfer process was 95.6 ± 2.0% (1SD, n=27 including sediment samples and reference materials).

Procedural blanks and standard reference materials were combusted to monitor combustion performance. Average procedural blank 1% $KMnO_4$ solutions yielded 0.10 ng Hg (± 0.01 ng Hg, 1SD, n=4) prior to transfer, and 0.13 ng Hg (± 0.02 ng Hg, 1SD, n=4) after transfer, representing <0.2% of sample solution Hg mass. Standard reference materials included NIST SRM 2711 (Montana Soil; 6.25 ± 0.19 μg g^{-1} THg) with an average recovery of 105.1 ± 0.1%

(1SD, n=2) and NIST SRM 1944 (NY/NJ Waterway Sediment; 3.4 ± 0.5 μg g^{-1} THg) with a recovery of 105.7% (n=1) relative to certified values.

2.3 Sequential Extractions

Five-step sequential extractions were performed on sieved streambed sediment collected from EFK 22.3, EFK 18.0, and EFK 8.7 to separate and quantify individual pools of sediment-bound Hg. We followed the sequential extraction procedure developed by Bloom *et al.*,[43] as this extraction method has been previously used to assess the forms of Hg in streambed sediment, stream bank soil, historical release deposits, biofilm, and floodplain soil of EFPC.[14,18,44-46] This sequential extraction procedure involved a series of five reagents of increasing chemical strength to extract operationally-defined pools of Hg, and included deionized water (F1), 0.1 M acetic acid (CH_3COOH) + 0.01 M trace metal grade HCl (F2), 1 M reagent grade KOH (F3), 12 M trace metal grade HNO_3 (F4), and aqua regia (F5) (see Section S2 in the Supporting Information for reagent preparation).[43] We are aware that suggestions have been made to further optimize the sequential extraction procedure, such as decreasing the concentration of the HNO_3 step[47] and decreasing the leach time.[48] However, to allow for the most direct comparison with previous sequential extraction studies in EFPC, we chose to maintain the original Bloom *et al.*[43] procedure.

Well-mixed sediment (but not ground) was weighed into 50-mL polypropylene centrifuge tubes (~0.4 g per tube), and the F1 reagent was added (~40 mL per tube), maintaining a 1:100 solid-to-liquid mass ratio. Because the F1 and F2 extractions were expected to release relatively small amounts of Hg, the contents of multiple centrifuge tubes (up to 2.4 g sediment with 240 mL reagent) were combined to yield enough Hg for isotope analysis. Centrifuge tubes were capped and rotated end-over-end for 21 ± 2 hours, then centrifuged for 20 minutes at 1560 rpm (450 x g). The supernatant was filtered using 0.45 μm cellulose nitrate filter cups (Nalgene) and poured into trace metal clean borosilicate glass bottles (Pyrex), combining the supernatant of multiple tubes representing the same sediment sample. An additional aliquot of the F1 reagent (~40 mL deionized water) was added to each centrifuge tube as a rinse step, which was then re-centrifuged, filtered, and added to the bottles. Extraction samples were brought to 1% BrCl and refrigerated, except for the F3 samples, which were brought to 5% BrCl, and some of the F5 samples, to which additional small aliquots of concentrated BrCl were later added until the

solution remained yellow after shaking. This process was repeated for the F2, F3, and F4 reagents, using the respective reagent for the rinse steps. After the addition of the F5 reagent (aqua regia, 10 mL HCl + 3 mL HNO_3), centrifuge tubes were briefly hand shaken, and then the loosely-capped tubes were stored in a fume hood for ~24 hours. The centrifuge tubes were then diluted to 40 mL with deionized water and filtered, and then additional deionized water was used for the rinse step. To prevent degradation of the cellulose nitrate filters while filtering the F3, F4, and F5 reagents, 40-80 mL of deionized water was added to the filter cup along with the reagents, diluting the extraction solutions. Brominated solutions were kept in the dark and refrigerated at 4ºC until analysis.

To quantify the amount of Hg leached from the sediment by each reagent, the THg concentration of each extraction solution was measured using CVAFS following EPA Method 1631.[42] To avoid matrix interferences from dissolved organic matter, an aliquot of each extraction solution was transferred to a 15-mL Teflon vial, diluted with 5% BrCl, and exposed to ultraviolet light for five to ten days prior to concentration analysis.[49,50] Samples were analyzed in batches with quality control including calibration verification standards, secondary standards, blanks, sample duplicates, and matrix spike recovery tests (see Section S1 in the Supporting Information for details). Procedural blanks, standard reference materials, and sample replicates were used to assess sequential extraction performance. Each of the five extractants were used for the procedural blanks, and average procedural blank solutions yielded 0.10 ng Hg (± 0.10 ng Hg, 1SD, n=20), typically representing <0.5% of sample solution Hg mass.

Sequential extraction experiments using pure Hg compounds have shown that individual forms of Hg are not always extracted by a single reagent and may be split into consecutively extracted fractions.[43,47,51] In addition, differing results within and between sequential extraction experiments[43,47] may be attributed to variations in Hg concentration, matrix material, particle size, or impurities in mineral composition.[52] For this study, rather than assigning specific Hg species to each extracted fraction, the five sequential extractions are thought of as a gradient of Hg compounds based on solubility and sorption properties, with some possible overlap between them (Figure S1). Throughout this paper, we use the phrases poorly soluble, strongly-bound, and recalcitrant to refer to the F4 and F5 sequential extractions, which likely contain mercuric sulfide and other poorly soluble Hg compounds.[43,47] For the middle of the gradient, we use the phrases organically-bound and intermediate solubility to refer to the F2 and F3 sequential extractions,

though we acknowledge that not all of the organically-bound Hg in the sediment is captured by these extractions, nor are these extractions capturing organically-bound Hg exclusively.[43,53] We use the phrases highly soluble, water-soluble, and weakly-bound to refer to the F1 sequential extractions, which likely contain a mixture of highly soluble Hg compounds, such as mercuric chloride and Hg bound to soluble organic matter, as well as readily exchanged sorbed forms of Hg.[37,43]

2.4 Sample Preparation for Isotope Analysis

Prior to isotope analysis, each sequential extraction sample was chemically reduced, and the resulting Hg(0) was purged from solution and re-oxidized in a 1% $KMnO_4$ trapping solution following previously described methods.[41] Briefly, aliquots of the already-brominated extraction samples were diluted to 1 L with deionized water and then further acidified (0.5% HCl) and oxidized (1% BrCl). Samples were then pre-reduced with 1.0 mL of 30% $HONH_3Cl$ and allowed to react for 1-2 hours. Samples were reduced with ~100 mL of 10% $SnCl_2$ (in 10% HCl), and Hg(0) was purged from solution with gold-filtered clean-laboratory air and subsequently trapped in a 5-10 g oxidizing solution of 1% $KMnO_4$. The 1% $KMnO_4$ trap solutions were later reduced with $HONH_3Cl$, and a small aliquot was analyzed for THg concentration using CVAFS following EPA Method 1631[42] as previously described for combustion solutions. Purge and trap recovery of Hg from extraction samples was 99.7 ± 3.6% (1SD, n=89 including sediment samples and reference materials). Purge and trap procedural blanks and standards (12, 15, or 35 ng Hg; NIST SRM 3133) were used to monitor analytical performance. Procedural blank 1% $KMnO_4$ solutions, yielding 0.22 ng Hg (± 0.44 ng Hg, 1SD, n=10, with one anomalously high value at 1.38 ng Hg), typically represented <1% of sample solution Hg mass. Procedural standard recovery was 98.3 ± 4.2% (1SD, n=21), and procedural standards were not significantly fractionated isotopically relative to NIST SRM 3133 bracketing standards (Table S2).

2.5 Mercury Isotope Analysis

Following Hg extraction and pre-concentration procedures, the Hg isotopic composition of each 1% $KMnO_4$ trap solution was measured using cold vapor multiple collector inductively coupled plasma mass spectrometry (CV-MC-ICP-MS; Nu Instruments) following previously described methods.[54,55] Thallium (NIST SRM 997) was used as an internal standard to correct for

instrumental mass bias, along with sample-standard bracketing with Hg standard NIST SRM 3133. On-peak zero corrections were applied to all masses.

Mass-dependent isotope fractionation (MDF) is reported as the permil (‰) deviation from the average of NIST SRM 3133 bracketing standards[55] using delta notation:

$$\delta^{xxx}Hg\ (‰) = ([(^{xxx}Hg/^{198}Hg)_{sample} / (^{xxx}Hg/^{198}Hg)_{NIST\ SRM\ 3133}] - 1) * 1000$$

where xxx is the mass of each Hg isotope between ^{199}Hg and ^{204}Hg. Mass-dependent fractionation is reported with $\delta^{202}Hg$ values. Mass-independent isotope fractionation (MIF) is reported as the difference between the measured $\delta^{xxx}Hg$ value and that which is theoretically predicted by the kinetic mass-dependent fractionation law,[55] using capital delta notation:

$$\Delta^{xxx}Hg\ (‰) \approx \delta^{xxx}Hg - (\delta^{202}Hg * \beta)$$

where xxx is the mass of each Hg isotope (^{199}Hg, ^{200}Hg, ^{201}Hg, and ^{204}Hg), and β is a constant for each isotope (0.252, 0.502, 0.752, 1.493, respectively).[55]

To characterize reproducibility of the mass spectrometry, each analytical session included 5 to 9 analyses of a secondary standard (UM-Almadén) at representative Hg concentrations (1 to 5 ng g^{-1}). We also measured the isotopic composition of each NIST SRM 3133 purge and trap standard once, and of each combustion reference material three times. To evaluate the external reproducibility and the accuracy of our results, we calculated the mean (± 2SE) for the collection of independent preparations of UM-Almadén and each reference material type (Table S2), and compared those means to the long-term average isotopic composition measured at the University of Michigan.[56] We represent the uncertainty in the isotopic composition of Hg in combustion samples with the average uncertainty (2SD) across combustion reference material analyses (Table S3, Table S4). We represent the uncertainty in the isotopic composition of Hg in sequential extraction samples with the average uncertainty (2SD) across all UM-Almadén analyses (Table S5, Table S6, Table S7).

2.6 Organic Carbon Analysis by Loss-on-Ignition

Organic carbon (OC) concentrations were determined following a loss-on-ignition (LOI) procedure[57] (Table S8). Sediment aliquots (~1.5 g) were taken from the same 2 g aliquots that had been ground for THg analysis (see Section 2.2) to ensure accurate calculation of THg per mass of organic carbon (μg THg g^{-1} OC) (Table S8). Sediment was weighed into disposable quartz fiber crucibles, which had been pre-baked in a muffle furnace at 800ºC for 12 hours. The

sediment was then heated to 105ºC for 12 hours to remove moisture, then 500ºC for 12 hours to release organic matter, and then 800ºC for 12 hours to release carbonates. The sediment was cooled to room temperature in a desiccator, and mass loss was measured after each 12-hour cycle. The percentage of mass loss after 500ºC was converted to a percentage of organic carbon by dividing the value by 2, based on the assumption that carbon makes up ~50% of organic matter.[58] Process blanks (pre-baked empty crucibles) and standard reference materials were used to monitor LOI performance. Mass loss from blanks was 0.08 to 0.46 mg (n=2) after 500ºC, representing <1% of average sample mass loss. Based on calculated percentages of organic carbon, NIST SRM 1944 (NY/NJ Waterway Sediment) had an average recovery of 99.6 ± 0.6% (n=2) relative to its certified %OC value of 4.4 ± 0.3%.

2.7 Statistical Analysis

All statistical analyses were conducted using publicly available Python packages. To assess whether there were significant differences in isotopic composition among sequential extraction fractions, we used a series of significance tests. First, we used two-tailed paired-samples t-tests (paired by size fraction) to assess whether there were significant offsets in isotopic composition between the F2 and F3 Hg fractions, and between the F4 and F5 Hg fractions, at each sampling site (Table S9). Given that the F2 and F3 fractions were isotopically similar, and that the F4 and F5 fractions were isotopically similar (see Section 3.4), we calculated the un-weighted average isotopic composition of the F2 and F3 Hg fractions (denoted as F2F3), and of the F4 and F5 Hg fractions (denoted as F4F5) for each sediment sample. We used paired samples t-tests with a Bonferroni adjustment for multiple comparisons to assess whether there were significant differences in isotopic composition among the F1, F2F3, and F4F5 Hg fractions (Table S10). Samples were paired by sediment size fraction within each site, such that F1, F2F3, and F4F5 were being compared within a single sediment sample. We also repeated this three-group comparison, but used the F3 Hg fraction in place of the F2F3 fraction (Table S11) in order to assess the influence of the F2 extraction samples which were analyzed at lower concentrations and tended to have higher within-site variability in isotopic composition than the other Hg fractions. Finally, we repeated these statistical assessments using independent sample averages (i.e., across all sediment size fractions within each site) and Tukey multiple comparisons tests (Table S12, Table S13). This was done to assess whether the results from our

paired within-size-fraction comparisons could be more generally applied to assess differences among sequential extraction fractions at a broader scale that would be more relevant to interpreting the influence of legacy Hg sources on the isotopic composition of pore water and surface water. We found similar outcomes regardless of whether we used significance tests on paired samples or independent samples (see Section 3.4).

To determine slopes for Δ^{199}Hg versus δ^{202}Hg and Δ^{199}Hg versus Δ^{201}Hg plots, the York regression was used, which incorporates uncertainty in the X and Y variables.[59] These slopes were generated using IsoplotR,[60] which requires 1SE as the error input term. For combustion samples this is represented by the average 1SE value across combustion reference material analyses, and for sequential extraction samples this is represented by the average 1SE value across all UM-Almadén analyses.

3. RESULTS & DISCUSSION

3.1 Assessment of Sequential Extraction Methods

Standard reference materials were used to assess the mass balance associated with the sequential extraction procedure. Based on the sum of the amount of Hg released in the five sequential extractions, NIST SRM 2711 had an average recovery of 95.4 ± 1.7% (1SD, n=3) and NIST SRM 1944 had a recovery of 102.3% (n=1) relative to certified values. The relative distribution of Hg fractions extracted from NIST SRM 2711 was reasonably similar to that reported by Bloom *et al.*[43] (Table S5). The calculated isotopic composition (THg_{calc}) of reference materials was based on the weighted average of sequential extraction Hg concentrations (Table S5). These values were within error of the isotopic composition obtained by combustion of bulk material (Table S2), and also agreed with the long-term average isotopic composition of the reference materials measured at the University of Michigan.[56] A comparison of the isotopic signatures associated with sequential extractions of NIST SRM 2711 across multiple studies is provided in the Supporting Information (see Section S3).

Total Hg concentrations and isotopic compositions of EFPC sediment samples obtained by the weighted average of sequential extractions also generally agreed with those obtained by whole sample combustion (Figure S2, Figure S4). However, the relative percent difference between average THg concentrations obtained from combustions and sequential extractions was larger for the 1-2mm size fraction (23.9 ± 12.7%, 1SD, n=3) than for the other three size

fractions (3.9 ± 2.5%, 1SD, n=9) (Figure S2). Additionally, only for the 1-2mm size fraction at EFK 22.3 did the THg concentration and isotopic composition significantly differ between the sample aliquots used for sequential extractions and each of the two combustion replicates (Figure S2, Figure S4a, Table S4, Table S6.1). These differences may have been due to greater heterogeneity within subsamples of this larger sediment size fraction, whereby individual grains of sediment with anomalous THg concentrations or isotope ratios may have had a stronger influence on the THg concentration and/or isotopic composition of the bulk sediment sample compared to smaller grain sizes.

The sequential extraction procedure was repeated two times for EFK 18.0: 250µm-1mm sediment (Table S7.1) and three times for NIST SRM 2711 (Table S7.2) to evaluate the variability in concentration and isotopic composition of the extracted Hg fractions. Partial sequential extraction replicates (only the first two extraction steps) were also performed on all size fractions of EFK 8.7 sediment as an additional evaluation of the variability within the F1 and F2 extraction steps (Table S7.1). Differences in δ^{202}Hg and Δ^{199}Hg values between sequential extraction replicates were within analytical uncertainty (14 of 16 replicates), except for δ^{202}Hg values of the F2 extraction replicates of NIST SRM 2711 (Table S7.2) and of the F1 extraction replicates for the EFK 8.7 250µm-1mm sediment (Table S7.1). Aside from these two anomalies, our sequential extraction replicates suggest that each sequential extraction was consistently targeting a specific pool of Hg that was isotopically similar across replicates and in some cases was isotopically distinguishable from other Hg pools.

When using a sequential extraction procedure to isolate Hg pools for isotopic analysis, it is important that the extraction procedure does not induce artificial isotope fractionation. This may be the result of incomplete dissolution/desorption of a target or non-target Hg pool. Based on kinetic fractionation mechanisms in which lighter isotopes react more quickly, it is expected that artificially induced isotope fractionation would result in lower δ^{202}Hg values in earlier extractions. In our sequential extractions, the only consistent offset in δ^{202}Hg was between the F4 and F5 pools, and the F4 pool had more positive δ^{202}Hg values (Figure S8) which is the opposite of what would be expected if this offset was caused by the extraction procedure itself. Additionally, Wiederhold *et al.*[36] demonstrated that partial dissolution of HgS and organically-bound Hg using 6 M HCl and 6 M HNO_3 did not result in isotope fractionation between the dissolved and residual fractions. A similar lack of fractionation has also been shown for iron

isotopes during dissolution of goethite, an iron oxide mineral, using 0.5 M HCl.[61] Overall, complete recoveries, consistent isotopic composition across sequential extraction replicates, and the apparent lack of artificial isotope fractionation suggests that the sequential extraction procedure used in our study was reliable for investigating the isotopic composition of individual operationally-defined pools of Hg within our sediment samples.

3.2 Mechanistic Controls on the Mercury Isotopic Composition of Streambed Sediment

Across all sampling sites, a majority (82-93%) of the sediment in the <2mm bulk samples had a diameter between 250μm and 2mm, while the 125-250μm and <125μm size fractions made up 2-4% and 5-14% of the bulk sediment, respectively (Table S1). Total Hg concentrations for EFPC streambed sediment ranged from 7.14 to 41.8 μg g^{-1} (based on combustion), with THg concentrations generally decreasing along the flow path for smaller size fractions and increasing along the flow path for larger size fractions (Figure S2, Table S3). These concentrations were similar to the range of sediment Hg concentrations reported in other recent studies of EFPC sediment,[14,32,45] and were much higher than those of regional background sites.[32]

Across all sites and sediment size fractions, EFPC streambed sediment δ^{202}Hg values ranged from -0.24‰ to 0.24‰ (± 0.09‰, 2SD) and Δ^{199}Hg values ranged from -0.12‰ to -0.05‰ (± 0.02‰, 2SD) based on combustion (Figure S5, Table S3). Associated Δ^{200}Hg and Δ^{204}Hg values were essentially zero, averaging 0.00‰ ± 0.01‰ (1SD, n=16) for both Δ^{200}Hg and Δ^{204}Hg (Table S3), suggesting minimal contribution of Hg to the sediment from precipitation or dry deposition.[41,62,63] This overall range in Hg isotope values is similar to that of streambed sediment samples reported previously for EFPC.[31,32] Across all sites and sediment size fractions, there were no overall trends in δ^{202}Hg or Δ^{199}Hg versus 1/THg (Figure S6), and when separated by size fraction, even the strongest trend was not statistically significant (smallest p-value for δ^{202}Hg vs. 1/THg was 0.082 for the <125μm size fraction). The lack of a relationship between isotope ratios and 1/THg concentration indicates that variations in THg concentration and isotopic signatures among sediment samples do not appear to be driven predominantly by the mixing of two isotopically distinct sources.

EFPC streambed sediment had a Δ^{199}Hg/δ^{202}Hg slope of -0.11 (± 0.01, 1SE, n=16) and a Δ^{199}Hg/Δ^{201}Hg slope of 1.37 (± 0.21, 1SE, n=16) (Figure S5). These slope values, as well as the relatively small magnitude of the measured Δ^{199}Hg values, suggest that mass-dependent and

nuclear volume-dependent fractionation effects may be partially responsible for the observed range in isotopic composition of the streambed sediment. Equilibrium mass-dependent fractionation causes shifts in δ^{202}Hg values due to the tendency of heavier Hg isotopes to be enriched in compounds with shorter, stiffer bonds (higher vibrational frequency).[64,65] Nuclear volume fractionation also causes shifts in δ^{202}Hg values due to the tendency of Hg isotopes with a larger nuclear radius (which are less strongly bound to electrons) to be enriched in compounds that give Hg a more positive partial charge.[64,65] For redox reactions, both of these isotope effects would result in higher δ^{202}Hg values in the oxidized Hg(II) phase, though these isotope effects also apply to non-redox reactions. Nuclear volume fractionation additionally causes shifts in Δ^{199}Hg and Δ^{201}Hg values, with a characteristic Δ^{199}Hg/Δ^{201}Hg ratio of ~1.5 to 1.6, due to the nuclear radius of Hg isotopes not scaling linearly with mass, with the two odd-numbered isotopes having smaller nuclear radii than what is expected based on the linear relationship between nuclear radius and mass for the five even-numbered isotopes.[65] Equilibrium mass-dependent fractionation and nuclear volume fractionation have been shown experimentally to cause equilibrium isotope effects during isotope exchange between liquid and gaseous Hg(0),[66,67] between coexisting Hg(II) species,[65,68] and between coexisting Hg(0) and Hg(II) species.[31,69] The results of these experimental studies have generally aligned with theoretical calculations of equilibrium fractionation factors[64,65,68,70] and have demonstrated Δ^{199}Hg/δ^{202}Hg slopes of -0.1 to -0.2 and Δ^{199}Hg/Δ^{201}Hg slopes of ~1.5 to 1.6. These values are within the range of uncertainty in the slopes for EFPC streambed sediment, suggesting that equilibrium isotope effects may at least partially account for the range in isotopic composition of the sediment.

Nuclear volume fractionation has also been shown to occur alongside kinetic mass-dependent fractionation, which causes shifts in δ^{202}Hg values due to the tendency of lighter Hg isotopes to react faster (due to their higher zero-point energy) and therefore be enriched in the products of a reaction.[71] Kinetic mass-dependent fractionation and nuclear volume fractionation have been shown to occur together during some kinetic reactions, such as evaporation of liquid Hg(0),[66] dark abiotic reduction of Hg(II),[72,73] and dark abiotic oxidation of Hg(0).[69] Similar to equilibrium reactions involving nuclear volume fractionation, these studies have also demonstrated Δ^{199}Hg/Δ^{201}Hg slopes of ~1.5 to 1.6, though the measured Δ^{199}Hg/δ^{202}Hg slopes have been shown to be more variable (both steeper and shallower) than those of equilibrium reactions. Importantly, experimental studies have shown that equilibrium isotope effects can

overwrite initial kinetic isotope effects as a reaction progresses, which can alter the $\Delta^{199}Hg/\delta^{202}Hg$ slope.[69]

Of the reactions mentioned above, some are more likely to have influenced the isotopic composition of EFPC streambed sediment than others. For example, of the 11 million kg of liquid Hg(0) historically used at Y-12, only ~0.3% was lost to the atmosphere,[10] and so evaporation of Hg(0) would not have caused significant isotope fractionation within the remaining liquid Hg(0). On the other hand, an estimated 1.2 ± 0.3% of the liquid Hg(0) historically used at Y-12 was oxidized and released directly to EFPC, mainly through a nitric acid washing procedure.[10] This process could have resulted in isotopic fractionation of the Hg(II) released to EFPC relative to the initial Hg(0) source. Dark abiotic oxidation of Hg(0), followed by isotope exchange between coexisting Hg(0) and Hg(II) species, has been experimentally shown to shift the oxidized Hg(II) phase toward more positive $\delta^{202}Hg$ and more negative $\Delta^{199}Hg$ values relative to the reduced Hg(0) phase.[69] In that study, the equilibrium isotope effect had overwritten the initial kinetic isotope effect (which initially had a steeper $\Delta^{199}Hg/\delta^{202}Hg$ slope), resulting in a $\Delta^{199}Hg/\delta^{202}Hg$ slope of -0.12 (± 0.01, 1SE, n=40) and a $\Delta^{199}Hg/\Delta^{201}Hg$ slope of 1.28 (± 0.19, 1SE, n=49) (or 1.62 ± 0.14, 1SE, n=49, if the regression analysis was forced through the origin).[69] This is consistent with the isotopic composition of EFPC streambed sediment, which primarily contains Hg(II) species, being offset toward higher $\delta^{202}Hg$ and lower $\Delta^{199}Hg$ values relative to the assumed isotopic composition of the historically used liquid Hg(0) (Figure 2). Although the exact isotopic composition of this historical liquid Hg(0) source is not known, commercial sources of liquid Hg(0) obtained from the major Hg mines around the world have an average $\delta^{202}Hg$ value of -0.38 ± 0.34‰ (1SD, n=13) and near-zero $\Delta^{199}Hg$.[74] Isotope fractionation by dark abiotic oxidation and equilibrium isotope effects could have largely occurred in the Y-12 facility during the nitric acid washing procedure. Once released from Y-12, much of the Hg(II) would have become associated with the streambed sediment through processes such as HgS precipitation, mineral sorption, and thiol ligand binding. Based on experimental studies, these processes may have shifted the isotopic composition of the sediment-bound Hg toward slightly lower $\delta^{202}Hg$ values, depending on what proportion of the Hg bound to the sediment[65,68,75,76] (Figure 2). Isotope fractionation by dark abiotic oxidation and equilibrium isotope effects could have also occurred (and could still be occurring) in the environment surrounding Y-12 where liquid Hg(0) was released to the soil through spills and leaks,[9] and

where Hg(0)-contaminated groundwater is known to enter the surface flow.[10] For *in situ* processes, however, there would need to be subsequent separation of the Hg(0) and Hg(II) phases, which could be achieved through preferential sorption of Hg(II) to sediment and/or volatilization of Hg(0). In addition to dark abiotic oxidation, equilibrium isotope effects between Hg(0) and Hg(II) species could also accompany Hg reduction processes, so long as the reduced Hg(0) does not volatilize immediately after being formed. For example, the isotopic composition of EFPC surface water suggests that photochemical reduction of Hg(II) is likely occurring along the flow path (see Section 3.6.2).[6] The coexisting Hg(0) and Hg(II) involved in Hg reduction processes could undergo equilibrium isotope exchange, which would shift the Hg(II) phase toward higher δ^{202}Hg and lower Δ^{199}Hg values. The Hg(II) could then be associated with the streambed sediment more so than the Hg(0) phase due to differences in sorption characteristics and/or volatilization of Hg(0).

Overall, it appears that equilibrium isotope effects that occur alongside Hg oxidation and reduction processes could have played an important role in determining the isotopic composition of the high-concentration streambed sediment within EFPC. Zheng *et al.*[69] stated that isotope exchange "could be ubiquitous" across a variety of biogeochemical reactions, including both oxidation and reduction reactions, which could alter isotopic signatures within ecosystems. Both Bartov[31] and Zheng *et al.*[69] pointed out that fractionation by isotope exchange reactions could overwrite initial fractionation by kinetic reactions. This could potentially make it difficult to deduce which kinetic reactions may have been dominant historically, especially for ecosystems in which both Hg oxidation and Hg reduction are possible. We suspect that equilibrium isotope effects may have the potential to set the "baseline" Hg isotopic composition for sediment and soil within ecosystems that contain both Hg(0) and Hg(II) species, including both non-contaminated and contaminated environments. In particular, it may be worth considering the potential impact of equilibrium isotope effects between Hg(0) and Hg(II) species for ecosystems with a known Hg(0) contamination source, such as within industrial sites and near Hg or gold mining sites. As an example, waterbodies downstream of several historical Hg mines in the California Coast Range have been impacted by Hg(II) and may also have been impacted by Hg(0) as a result of losses during on-site HgS ore roasting processes.[77,78] One such waterbody is Cache Creek, for which an investigation of the isotopic composition of the sediment revealed a Δ^{199}Hg/δ^{202}Hg slope of -0.12 (± 0.02, 1SE, n=11) and a Δ^{199}Hg/Δ^{201}Hg slope of 1.69 (± 0.34,

1SE, n=11).[79] These slope values, along with the lack of a relationship between Hg isotope ratios and 1/THg concentration, suggest that the isotopic composition of the sediment has been influenced by biogeochemical reactions involving mass-dependent fractionation and nuclear volume fractionation, which could include equilibrium isotope effects between Hg(0) and Hg(II) species.

3.3 Sequential Extractions: Mercury Concentrations

Across all sites and size fractions, a majority of the Hg was strongly bound to the sediment, found mostly in the F4 and F5 fractions, which together made up 94.6 ± 5.2% (1SD, n=12) of the THg (Figure 3, Table S6). The F3 fractions were the next largest, which made up a larger percentage of THg at the downstream site than at the two upstream sites (5.3 to 20.5% at EFK 8.7, compared to 1.7 to 2.5% at EFK 18.0 and 1.5 to 3.8% at EFK 22.3) (Figure 3, Table S6). These higher proportions at EFK 8.7 were driven by higher concentrations of Hg in the F3 fractions across all sediment grain sizes, as well as an especially low THg concentration for the 125-250μm size fraction (Table S6). Note that methylmercury typically makes up <0.05% of THg within EFPC streambed sediment[14,15,45,80] and thus would typically represent <3% of the F3 Hg fraction. The F1 fractions made up 0.7 ± 0.4% (1SD, n=12) of the THg, and the proportion of the F2 fractions was even smaller. The relative proportions among these Hg fractions, as well as the increasing proportion of the F3 fraction along the flow path, aligns with observations by Brooks *et al.*[14] using the same sequential extraction method on EFPC streambed sediment.

Despite the higher proportions and higher concentrations of Hg in the F3 fractions at EFK 8.7 (Table S6.3), which are thought to primarily represent organically-bound Hg, the organic carbon concentrations of the sediment generally decreased along the flow path (Table S8), accentuating increases in the ratio of F3-extracted Hg to organic carbon along the flow path. At the two upper sites (EFK 22.3 and EFK 18.0), the amount of Hg in the F3 fractions (Hg_{F3}) relative to the organic carbon (OC) content of the sediment was consistent across all sediment size fractions, averaging 26.0 ± 7.1 μg Hg_{F3} g^{-1} OC (1SD, n=8). This concentration increased substantially for all but the smallest size fraction at EFK 8.7, averaging 197 ± 35 μg Hg_{F3} g^{-1} OC (1SD, n=3) (Figure S7, Table S8). This 7.6-fold increase in the Hg_{F3}:OC ratio was driven by both an increase in the Hg_{F3} concentration of the sediment (Table S6) as well as a decrease in the organic carbon concentration (Table S8), and suggests that the Hg content of the organic matter

within the streambed sediment generally increases downstream, though the explanation for this trend is unclear.

3.4 Sequential Extractions: Mercury Isotopic Composition

Across all sequential extractions of EFPC streambed sediment, δ^{202}Hg values ranged from -0.64‰ to 0.49‰ (± 0.08‰, 2SD) and Δ^{199}Hg values ranged from -0.16‰ to 0.04‰ (± 0.05‰, 2SD) (Figure 4, Figure S4, Table S6). Sequential extractions had a Δ^{199}Hg/δ^{202}Hg slope of -0.15 (± 0.01, 1SE, n=60) and a Δ^{199}Hg/Δ^{201}Hg slope of 1.57 (± 0.16, 1SE, n=60) (Figure S3). As with the bulk sediment, Δ^{200}Hg and Δ^{204}Hg values of the sequential extractions were essentially zero, averaging 0.00‰ ± 0.02‰ (1SD, n=60) for both Δ^{200}Hg and Δ^{204}Hg (Table S6), suggesting minimal contribution of Hg to any of the individual sediment Hg fractions from precipitation or dry deposition.[41,62,63]

In general, the F2 and F3 Hg fractions had a positive offset in Δ^{199}Hg values relative to the other sediment Hg fractions (Figure 4, Figure S8). For each of the three sampling sites, the isotopic composition of the F2 and F3 Hg fractions within individual sediment size fractions were similar to one another (Figure S8), as the mean offsets in δ^{202}Hg and Δ^{199}Hg values between the F2 and F3 fractions for each site were not significantly different from zero (Table S9). Results of pairwise comparisons between the F4 and F5 Hg fractions within individual size fractions were more variable. The mean offset in Δ^{199}Hg values between the F4 and F5 Hg fractions for each site ranged from 0.00 ± 0.02‰ to -0.01 ± 0.02‰ (Figure S8), indicating no significant difference within individual size fractions at either EFK 22.3 or EFK 18.0 (Table S9). Although our statistical analyses did suggest that there was a difference in Δ^{199}Hg values between F4 and F5 fractions at EFK 8.7, this appeared to be driven by an exceptionally small mean offset and standard deviation (-0.01 ± 0.00‰) (Table S9), and thus we deemed differences in Δ^{199}Hg values between the F4 and F5 Hg fractions to be negligible overall. The mean offset in δ^{202}Hg values between F4 and F5 Hg fractions was more variable (Figure S8), increasing from 0.16 ± 0.12‰ (p=0.075, n=4) at EFK 22.3 to 0.34 ± 0.07‰ at EFK 8.7 (p=0.002, n=4) (Table S9). Nonetheless, based on their similarity in Δ^{199}Hg values, we chose to combine the F4 and F5 Hg fractions for our subsequent assessments. This approach was further supported by our unpaired tests of F2 vs. F3 Hg fractions, and F4 vs. F5 Hg fractions, within each sampling site which indicated that neither F2 and F3, nor F4 and F5, could be consistently resolved from one

another at the streambed level (i.e., across all size fractions within each site) (Table S12). This becomes important when tracking sources through the stream ecosystem.

Based on the isotopic similarity of the F2 and F3 Hg fractions, and the F4 and F5 Hg fractions, we calculated the un-weighted average isotopic composition of the F2 and F3 fractions (hereafter, F2F3) and of the F4 and F5 fractions (hereafter, F4F5) for each sediment sample (Figure 5). We then made a three-group comparison of means among the F1, F2F3, and F4F5 Hg fractions using data paired within individual sediment size fractions (Table S10), as well as with unpaired data within each site (Table S13). One key result was that the F1 and F4F5 Hg fractions were statistically indistinguishable at all three sites, in terms of both δ^{202}Hg and Δ^{199}Hg values, using paired and unpaired data (Table S10, Table S13). The F1 Hg fraction was also similar to the F2F3 Hg fraction with respect to δ^{202}Hg values, for both paired and unpaired data, driven in part by the high variability in the F2F3 δ^{202}Hg values (Table S10, Table S13). However, the F1 Hg fraction differed from the F2F3 Hg fraction with respect to Δ^{199}Hg values at our site furthest upstream, EFK 22.3, but the Δ^{199}Hg values of these Hg fractions were not significantly different at EFK 18.0 or EFK 8.7, in terms of both paired and unpaired data, as F2F3 Δ^{199}Hg values decreased along the flow path (Figure 5, Table S10, Table S13). The F2F3 Hg fraction δ^{202}Hg and Δ^{199}Hg values also were significantly offset from F4F5 δ^{202}Hg and Δ^{199}Hg values paired within individual size fractions at EFK 22.3 (Table S10), although using unpaired data δ^{202}Hg values of the F2F3 and F4F5 fractions were not significantly different at EFK 22.3 (Table S13). Along the flow path, F2F3 δ^{202}Hg values increased and Δ^{199}Hg values decreased (Figure 5, Table S13), becoming indistinguishable from F4F5 values paired within individual sediment size fractions (Table S10). Although these patterns of convergence in F2F3 and F4F5 Hg fractions were not observed for δ^{202}Hg values at the streambed level (i.e., because δ^{202}Hg values of F2F3 fractions did not statistically differ from F4F5 at EFK 22.3 using unpaired data), this convergence between F2F3 and F4F5 Hg fractions remained strong with respect to Δ^{199}Hg values compared at the streambed level, that is, across all sediment size fractions at each site (Table S13). Thus, a second key result was that overall the isotopic composition of the F2F3 Hg pool in the sediment appeared to converge with that of the F1 and F4F5 Hg pools along the flow path.

We note that this convergence in isotopic composition of F2F3 Hg pools with F1 and F4F5 Hg pools was partially driven by high variability in the isotopic composition of the F2 Hg fraction, which is consistent with the concept of small Hg pools being more easily isotopically

fractionated relative to large pools. When we excluded the F2 Hg fractions from this analysis, the support for converging isotopic compositions along the flow path was somewhat weakened. Without F2 included in our paired samples statistical model, the F3 Hg fractions consistently had a significantly positive mean offset in Δ^{199}Hg values relative to both the F1 and F4F5 Hg pools at all three sites, although these differences did decline in magnitude along the flow path, as supported by concomitantly increasing p-values (Table S11). Nonetheless, the remainder of our discussion is based on the complete dataset, including the F2 Hg fractions, and suggests that (*i*) the F1 and F4F5 Hg pools have similar isotopic compositions throughout all sediment size fractions at all sites, and (*ii*) the isotopic composition of the F2F3 Hg pool appears to converge with that of the F1 and F4F5 Hg pools along the flow path, especially with respect to Δ^{199}Hg values.

3.5 Sediment as a Potential Source of Dissolved Mercury to Stream Water

3.5.1 Weakly-bound mercury in sediment may be derived from more recalcitrant pools. In our sequential extractions, the weakly-bound F1 sediment Hg fractions were isotopically more similar to the strongly-bound F4F5 Hg fractions than to the moderately-bound F2F3 Hg fractions (Figure 4, Table S10). One possible explanation is that within the streambed sediment, poorly soluble high-concentration Hg pools (F4F5) may slowly release dissolved Hg into the pore water, some of which may subsequently re-adsorb onto the sediment as a weakly-bound pool (F1). This weakly adsorbed Hg could accumulate on the sediment, retaining its isotopic composition and later be released to the stream water.

Poorly soluble Hg pools in the streambed sediment, likely made up largely of HgS, can be partially released if sulfide is replaced with dissolved organic matter with high aromaticity,[22,23] or by oxidative dissolution by high levels of dissolved oxygen[25-27] or with the help of sulfur-oxidizing bacteria.[24] Several laboratory experiments have also demonstrated re-adsorption of Hg onto HgS minerals,[25-27,81] as well as adsorption of Hg onto sediment and soil which have a variety of different sorption sites with varying affinities for Hg.[82,83] Although Hg re-adsorbed onto HgS would be relatively strongly bound,[84] Hg that has re-adsorbed onto weaker sorption sites within the sediment could potentially be represented in the F1 sediment extractions. Additionally, after performing leaching experiments on EFPC stream bank soil, Peterson *et al.*[18] suggested that differences in the amount of Hg released during their experiments

might have been due to re-adsorption of Hg onto soil particles. Zhang *et al.*[85] also saw evidence of re-adsorption of Hg after it had been released from EFPC streambed sediment. These studies lend support to our suggestion that dissolution of small amounts of HgS and other Hg compounds, followed by re-adsorption of Hg(II) onto the sediment and eventual re-release of the weakly-bound Hg into the stream water, could be part of a mechanism by which sediment-bound legacy Hg contributes dissolved Hg to the stream. This could explain why weakly-bound Hg in the sediment (represented by the F1 extraction) is not completely depleted over time, but rather may be replenished by the release of strongly-bound Hg from more recalcitrant compounds that are subsequently re-adsorbed to the sediment.

One key assumption within our hypothesis that weakly-bound Hg within the sediment (F1 pool) is derived from the more abundant recalcitrant Hg (F4F5 pool), is that the processes involved do not induce significant isotope fractionation. To our knowledge, no study has assessed the isotopic fractionation that may be associated with processes that remobilize Hg within recalcitrant Hg compounds (e.g., DOM dissolution of HgS).[86] Although kinetic and equilibrium reactions typically result in isotope fractionation,[30] dissolution of minerals occurs only at the surface of the mineral, and this limits the possibility of large isotope fractionation effects.[61] Extraction experiments also suggest that recalcitrant Hg pools could be partially dissolved without fractionation. For example, Wiederhold *et al.*[36] showed that partial dissolution of HgS and organically-bound Hg using 6 M HCl and 6 M HNO_3 resulted in no measurable Hg isotope fractionation. Additionally, in sequential extractions performed on unroasted HgS ore, small water-soluble Hg pools were isotopically similar to the bulk material.[34] Brocza *et al.*[37] suggested that the extent to which various sequential extraction experiments have found isotopically distinct fractions of Hg within solid samples appears to be highly dependent on site-specific Hg speciation and spatial heterogeneity. In sequential extractions performed on contaminated soils and calcine waste from Hg mining sites, water-soluble Hg fractions tended to be isotopically heavier than recalcitrant Hg,[33-35] but in another study involving sequential extractions of soil and sediment downstream of an industrial facility, water-soluble Hg fractions were found to be isotopically similar to recalcitrant Hg.[38] Additionally, for sequential extractions performed on soil core samples from a $HgCl_2$-contaminated industrial site, water-soluble Hg fractions tended to be isotopically heavier than recalcitrant Hg for soil samples with the highest THg concentrations and the largest relative proportions of more mobile forms of Hg. However,

for samples with lower THg concentrations that were dominated by recalcitrant forms of Hg, water-soluble Hg fractions tended to be isotopically similar to recalcitrant Hg.[37] Although some of the evidence provided here may be site-specific, these results suggest that within EFPC, where the streambed sediment is dominated by HgS[18,19] and other recalcitrant forms of Hg (F4+F5 make up 94.6 ± 5.2% of THg, 1SD, n=12), dissolution of recalcitrant Hg could plausibly occur without inducing significant isotope fractionation.

Adsorption of dissolved Hg onto solid minerals has been experimentally shown to induce isotope fractionation by enriching the adsorbed Hg in lighter isotopes relative to the dissolved phase.[68] This fractionation is hypothesized to be the result of equilibration between neutral and positively charged Hg(II) complexes, in which positively charged complexes are generally isotopically lighter and have a higher affinity for binding onto surfaces than neutral complexes. However, as the fraction of adsorbed Hg approaches 100%, the degree of fractionation decreases until the isotopic composition of the adsorbed phase matches that of the original dissolved Hg.[68] Several experimental studies have demonstrated that adsorption of Hg onto solid HgS[25-27,81] and onto contaminated and non-contaminated sediment and soil[82,83,85] can occur rapidly and, in some cases, nearly completely. This suggests that subsequent to dissolution of small portions of HgS and other Hg minerals, rapid re-adsorption could feasibly occur without significant isotope fractionation. This re-adsorbed Hg would likely be released during different steps within the sequential extraction procedure, with Hg re-adsorbed to weak sorption sites potentially being released in the F1 extraction. This could explain the similarity in isotopic composition of our F1 and F4F5 sediment Hg fractions. Additional studies that investigate the isotope fractionation involved with partial dissolution of HgS, and re-adsorption of Hg onto HgS and other sorption sites within sediment, will be required to further assess this hypothesis.

3.5.2 Comparison of sequential extractions, surface water, and pore water. While the proportions of Hg released by the F1 extractions were small (Table S6), this amount is not insignificant. Based on dissolved Hg flux measurements[29] and previous sequential extractions of EFPC streambed sediment,[14] Demers *et al.*[6] calculated that the release of the water-soluble fraction of Hg in the streambed (i.e., the F1 pool) would be enough to sustain the annual dissolved Hg flux to the surface water, so long as the water-soluble fraction in the sediment is replenished. Demers *et al.*[6] further suggested that soluble pools of Hg in the sediment could be replenished by stream bank erosion, however sequential extractions of EFPC stream bank soil

later revealed that the proportion of water-soluble Hg in bank soil was even lower than the proportion of water-soluble Hg in streambed sediment.[17] Weakly-bound Hg in the streambed sediment could also potentially be replenished by the contaminated stream water flowing over the sediment, although this would not represent a net flux of dissolved Hg to the surface water, as has been observed.[6,13] Moreover, dissolved Hg in the surface water near our sampling sites consistently had positive Δ^{199}Hg values (Figure 6),[6] while the F1 sediment Hg fractions had negative Δ^{199}Hg values, suggesting that surface water is not the primary contributor of weakly-bound Hg in the sediment. Instead, the results of this study suggest that the weakly-bound Hg in the sediment could be derived from and replenished by the more abundant recalcitrant fractions in the sediment, which would be a sustainable source for many years. This finding, along with the similarities in isotopic composition between the F1 and F4F5 Hg pools, suggests that small amounts of strongly-bound Hg may continuously be remobilized, contributing to both the weakly-bound Hg pools in the sediment and to the dissolved Hg in the stream water.

Previous Hg flux measurements have revealed that between EFK 23.4 and EFK 5.0, diffusive legacy sources contribute 6 to 36% of the total dissolved Hg flux, depending on hydrologic connectivity.[6,13] In a previous Hg isotope study at EFPC, Demers *et al.*[6] suggested that hyporheic pore water contributes to this dissolved Hg flux and influences the isotopic composition of the surface water, increasing its δ^{202}Hg values along the flow path. In that study, hyporheic pore water samples with the highest dissolved Hg concentrations tended to have negative Δ^{199}Hg values and relatively higher, positive δ^{202}Hg values, while surface water and low-concentration pore water samples tended to have positive Δ^{199}Hg values and relatively lower, negative δ^{202}Hg values (Figure 6). It is possible that these high-concentration pore water samples contained remobilized legacy Hg released from the sediment, leading to their high dissolved Hg concentrations and isotopic signatures that were shifted toward those of the F1, F4, and F5 Hg pools in the sediment. Additionally, at the two upstream sites (EFK 22.3 and EFK 18.0), δ^{202}Hg values of the F1 sediment Hg fractions were near-zero or slightly negative, while at the downstream site (EFK 8.7), δ^{202}Hg values of the F1 Hg fractions were near-zero or slightly positive (Figure 4, Figure S4). Thus, weakly-bound Hg in the streambed sediment and hotspots of dissolved Hg in the hyporheic pore water may contribute to the flux of dissolved Hg entering the surface water in a matter that is consistent with the observed increase in δ^{202}Hg values of the

surface water dissolved phase along the flow path, which aligns with the interpretations made by Demers *et al*.[6]

3.6 Interactions between Sediment and Biofilm

3.6.1 Biofilm and suspended particulates as sources of organically-bound mercury to the streambed sediment. The F2 and F3 Hg fractions within each sediment size fraction, which had similar Hg isotopic compositions to one another (Table S9), were likely dominated by organically-bound Hg.[43] Suspended particulates within EFPC have been found to be largely composed of diatoms and mineral particles coated with organic matter,[87] so suspended particulates are one likely source of organic matter and organically-bound Hg to the streambed sediment. Another likely source is the nearly-ubiquitous streambed biofilm layer within EFPC, which may be incorporated into the sediment as it goes through cycles of growth and decay and is washed downstream, making it a continuous source of organic matter and organically-bound Hg to the sediment.

The Hg concentration of the F2F3 Hg fractions (Hg_{F2F3}) across all sediment samples ranged from 0.30 to 1.72 μg Hg_{F2F3} g^{-1} sediment, which accounted for 1.6 to 21% (median = 2.6%) of the THg measured (n=12) (Table S6). When normalized to the organic carbon content of each sediment sample, the concentration of the F2F3 Hg fractions ranged from 15.5 to 237 μg Hg_{F2F3} g^{-1} OC, with a median value of 32.1 μg Hg_{F2F3} g^{-1} OC (values for Hg_{F2F3} are similar to Hg_{F3} in Figure S7, Table S8). In comparison, a previous study found that the concentration of the F2F3 Hg pools in EFPC streambed biofilm ranged from 2.23 to 4.95 μg Hg_{F2F3} g^{-1} biofilm, which accounted for 15 to 25% (median = 16%) of the THg measured (n=4).[45] Organic carbon concentrations were not measured for this small set of biofilm samples, but a larger and more recently collected EFPC biofilm sample set was found to consist of an average of 11.7 ± 6.1% organic carbon (1SD, n=64, measured via loss-on-ignition). For reference, the larger set of biofilm samples that were analyzed for organic carbon had an average THg concentration of 9.2 ± 6.6 μg THg g^{-1} biofilm (1SD, n=64), and the smaller set of biofilm samples that had been used for sequential extractions had an average THg concentration of 22.9 ± 9.5 μg THg g^{-1} biofilm (1SD, n=4).[45] While not a perfect comparison, we used these two sample sets to calculate the concentration of the F2F3 Hg pools in biofilm normalized to the average organic carbon content, which ranged from 19.1 to 42.2 μg Hg_{F2F3} g^{-1} OC, with a median value of 24.7 μg Hg_{F2F3} g^{-1} OC.

These concentrations within the biofilm appear to be high enough that a significant portion of the F2F3 Hg pool in the sediment could have been derived from the streambed biofilm layer.

The F2 and F3 sediment-bound Hg pools in this study had isotopic compositions similar to the EFPC biofilm and suspended particulates analyzed by Demers *et al.*[6] at each site along the stream (Figure 7). As previously reported, the isotopic composition of biofilm and suspended particulates shifted along the flow path, with increasing δ^{202}Hg and decreasing Δ^{199}Hg values that converged with the isotopic composition of <125μm streambed sediment.[6,32] These trends are similar to the shifts in isotopic composition of our F2F3 Hg pool toward that of the F1 and F4F5 Hg pools along the flow path, as determined through statistical analyses (Figure 5, Figure 7, Table S10) (see Section 3.4). This similar shift in isotopic composition further suggests that the F2 and F3 Hg pools in the sediment may have been derived from biofilm and/or suspended particulates. Note that methylmercury typically makes up <0.2% and <0.05% of THg within EFPC biofilm and streambed sediment, respectively,[14,15,45,80] which translates to methylmercury making up <1.3% and <3% of the F2F3 Hg fractions within biofilm and streambed sediment, respectively. Thus, while methylation and demethylation reactions may induce isotope fractionation in the pool of methylmercury within the biofilm and sediment, these reactions are not likely to be responsible for the shift in isotopic composition of the biofilm or the F2 and F3 sediment Hg pools along the flow path.

Altogether, the concentration of the F2F3 Hg fraction (normalized to organic carbon content) in biofilm relative to streambed sediment, as well as the similarity in the isotopic composition of biofilm, suspended particulates, and the F2 and F3 sediment Hg fractions, suggests that biofilm and/or suspended particulates are likely sources of organically-bound Hg to the sediment and are responsible for the shift in isotopic composition of the F2 and F3 sediment Hg pools along the flow path (Figure 7). This hypothesis relies on the assumption that the organically-bound Hg pool (F2F3) within biofilm and suspended particulates is isotopically similar to bulk biofilm and suspended particulates, which has not been assessed and will require further study.

3.6.2 Mechanisms influencing the mercury isotopic composition of biofilm and suspended particulates. Demers *et al.*[6] proposed that the shift in Hg isotopic composition of EFPC biofilm and suspended particulates along the flow path (i.e., toward higher δ^{202}Hg values and slightly lower Δ^{199}Hg values) could result from suspended particulates being modified as

they move downstream by a process similar to nutrient spiraling,[88] being repeatedly deposited into the streambed biofilm layer where photochemical and microbial Hg reduction processes could alter their isotopic composition before being re-suspended. This combination of reactions was proposed to explain the shift in isotopic composition of suspended particulates and biofilm along the flow path while simultaneously accounting for the observed transient increases in Δ^{199}Hg values of the surface water dissolved phase,[6] which may have resulted from the pulsed release of Hg(0) (with relatively higher Δ^{199}Hg values) to the dissolved phase from the suspended particulates and/or biofilm by photochemical reduction of thiol-bound Hg(II) along the stream.[89] This combination of reactions was also proposed based on the observed Δ^{199}Hg/Δ^{201}Hg slope of 0.98 (± 0.18, 1SE, n=24) for suspended particulates,[6] which aligns with the experimentally determined Δ^{199}Hg/Δ^{201}Hg slope of 1.0 to 1.3 for photochemical reduction of Hg(II).[72,89,90] The slope of 0.98 for suspended particulates was obtained using the ordinary least squares regression,[6] although by using the York regression, which accounts for uncertainty in both the X and Y variables,[59] the Δ^{199}Hg/Δ^{201}Hg slope value for suspended particulates is calculated to be 1.33 (± 0.27, 1SE, n=24). Although this higher value is still within the range of experimentally determined slopes for photochemical reduction, especially given that all Δ^{199}Hg and Δ^{201}Hg values were ≤ 0.3‰,[30] it opens up the possibility that processes involving nuclear volume fractionation, which typically have a Δ^{199}Hg/Δ^{201}Hg slope of 1.5 to 1.6,[65,67,69,70,72,73] could also have influenced the isotopic composition of the suspended particulates. Additionally, the Δ^{199}Hg/δ^{202}Hg slope for suspended particulates was -0.11 (± 0.03, 1SE, n=24).[6] These slopes are very similar to the slope values for bulk streambed sediment in this study (Figure S9), which we propose were likely driven by equilibrium isotope effects between coexisting Hg(0) and Hg(II) species[69] (see Section 3.2). Based on these similar slopes, as well as the convergence in δ^{202}Hg and Δ^{199}Hg values of the suspended particulates and biofilm with those of the streambed sediment,[6] we offer an overall simpler explanation for the evolution of the isotopic composition of suspended particulates and biofilm along the flow path. We suggest that this shift is simply due to mixing with fine-grained streambed sediment, which could account for the relatively large increase in δ^{202}Hg values of the suspended particulates and biofilm along the flow path, negating the need for microbial Hg reduction in the previous explanation (which shifts the oxidized phase toward higher δ^{202}Hg values). Mixing with streambed sediment could also account for the small decrease in Δ^{199}Hg values along the flow path, although photochemical reduction of thiol-bound

Hg(II) in the particulate phase would still be required to explain the transient increased in Δ^{199}Hg values of the surface water dissolved phase.

3.6.3 Evidence for the transfer of weakly-bound mercury from streambed sediment to biofilm and suspended particulates. Within the streambed sediment, the F2F3 pools of Hg also increased in δ^{202}Hg and decreased in Δ^{199}Hg values along the flow path, converging with the isotopic composition of the F1 and F4F5 sediment Hg pools (Figure 4, Figure 5). Physical incorporation of fine sediment grains into the biofilm and suspended particulates would primarily contribute recalcitrant forms of Hg, potentially altering the isotopic composition of these materials. Physical mixing with sediment, however, would likely not have significantly altered the isotopic composition of the organically-bound Hg pools within the biofilm and suspended particulates. Thus, we would not expect subsequent incorporation of biofilm and suspended particulates into the streambed sediment to alter the isotopic composition of the F2F3 sediment Hg pools along the flow path. However, relatively weakly-bound Hg (i.e., from the F1 pool), which itself may be derived from the more recalcitrant F4F5 pools (see Section 3.5.1), could have been dissolved and transferred into biofilm and suspended particulates where it may have become bound to organic ligands. Then, as biofilm and suspended particulates became physically incorporated into the streambed sediment along the flow path, this organically-bound Hg could have been contributed to the F2F3 sediment Hg pools. This would have caused the F2F3 Hg pools in the sediment to become isotopically more similar to recalcitrant forms of Hg, and thus could explain the convergence in isotopic composition of the F2F3 Hg pool with the F1 and F4F5 Hg pools within the streambed sediment along the flow path (Figure 4, Figure 5).

This explanation of F2F3 isotopic convergence with F1 and F4F5 Hg pools in the streambed sediment would also require no (or net zero) isotope fractionation during the transfer of weakly-bound (F1) Hg from sediment to biofilm and suspended particulates, and the re-incorporation of Hg from biofilm and suspended particulates into the organically-bound (F2F3) sediment Hg pool. While this seems somewhat unlikely, the fractionation that results from this process is difficult to predict without knowing the chemical form of weakly-bound Hg in the sediment. Regardless of potential fractionation, the near-quantitative transfer of small pools of Hg from the F1 to the F2F3 fraction could be achieved with no *net* fractionation. Additionally, the physical incorporation of biofilm and suspended particulates into the streambed along the

flow path, which would contribute organically-bound Hg to the F2F3 pool in the sediment, would not be expected to induce isotope fractionation.

Overall, we suggest that physical mixing with fine-grained streambed sediment (along with photochemical reduction of thiol-bound Hg(II)) could explain the shifts in isotopic composition of the bulk biofilm and suspended particulates along the flow path. At the same time, our sequential extraction data suggest that the F2F3 Hg pools in the streambed sediment likely originate from organically-bound Hg in biofilm and suspended particulates, and that dissolution and transfer of weakly-bound (F1) Hg from the sediment to the biofilm and suspended particulates, followed by re-incorporation into the organically-bound (F2F3) sediment Hg pool, could explain the shifts in isotopic composition of the F2F3 sediment Hg pools along the flow path. However, to evaluate the likelihood of this scenario, more process-specific experimental isotope fractionation studies will need to be undertaken to identify the biogeochemical processes involved and the potential fractionation that each process may or may not induce.

4. CONCLUSIONS & IMPLICATIONS

In this study, we measured THg concentrations and Hg isotope ratios in four size fractions of streambed sediment collected from four sites along East Fork Poplar Creek, and also performed five-step sequential extractions and Hg isotope analyses on sediment from three of these sites. We found that there were no significant correlations between isotope ratios and THg concentration for any of the sediment size fractions, suggesting that variations in THg concentration and isotopic signatures were not driven by mixing between two sources with distinct Hg concentrations and isotopic compositions. Instead, based on the $\Delta^{199}Hg/\Delta^{201}Hg$ and $\Delta^{199}Hg/\delta^{202}Hg$ slope values for streambed sediment, we suggest that the isotopic composition of the sediment appears to have been influenced by equilibrium reactions involving nuclear volume fractionation, including equilibrium isotope exchange between coexisting Hg(0) and Hg(II) species. The isotope fractionation imparted on the sediment by equilibrium isotope effects may have over-printed that of kinetic Hg oxidation and reduction reactions, such as oxidation of metallic Hg(0) prior to and after being released from Y-12, as well as *in situ* reduction of Hg(II) within the stream. The equilibrium isotope effect appears to control the overall isotopic composition of the recalcitrant Hg pool throughout the stream ecosystem (Figure 2). The results

of our study provide an *in situ* ecosystem-based example of how equilibrium isotope effects may have over-printed isotope fractionation signatures imparted by kinetic oxidation and reduction reactions, as hypothesized by Bartov[31] and later observed experimentally by Zheng *et al*.[69] Equilibrium isotope effects between redox species may be especially relevant for ecosystems that have been contaminated with both Hg(0) and Hg(II), such as industrial and mining sites.

Similar to previous studies,[14,45] our sequential extractions showed that recalcitrant forms of Hg make up a majority of the Hg in EFPC streambed sediment, followed by Hg compounds of intermediate solubility such as organically-bound Hg, and small but significant amounts of weakly-bound Hg (Figure 3, Table S6). The similarity in isotopic composition between the F1 and F4F5 sediment Hg fractions suggests that the weakly-bound pool may be derived from the strongly-bound legacy Hg through dissolution and rapid re-adsorption to the sediment. This implies that weakly-bound Hg pools in the sediment may continually be replenished by the large reservoir of recalcitrant Hg in the streambed, which itself is also replenished by stream bank erosion,[15,16] suggesting that the streambed sediment will likely be a source of dissolved Hg for many years. Dissolution of legacy Hg from streambed sediment can help explain the isotopic composition of hyporheic pore water samples with high dissolved Hg concentrations, which had higher δ^{202}Hg values and lower Δ^{199}Hg values than surface water and low-concentration pore water,[6] and appeared to be influenced by the F1, F4, and F5 Hg pools in the streambed sediment (Figure 6). The elevated δ^{202}Hg values of the high-concentration pore water, as well as the increase in δ^{202}Hg values of the F1 sediment Hg fractions along the flow path (Figure 4), align with the increasing δ^{202}Hg values of the surface water dissolved phase along the flow path.[6] This suggests that hyporheic pore water and weakly-bound sediment Hg pools are likely sources of dissolved Hg to the surface water, contributing to the diffuse Hg flux which makes up 6 to 36% of the total dissolved Hg flux along the stream.[6,13] Together, these isotope data and flux measurements suggest that even if the upstream point-source were to cease delivering dissolved Hg to the stream, dissolved Hg concentrations in the surface water would likely remain elevated due to the release of dissolved Hg from the streambed. The slow release of dissolved Hg from seemingly recalcitrant legacy sources may be common among other legacy Hg-contaminated stream ecosystems, and should be considered when evaluating the potential for ecosystem recovery from historical Hg inputs.

Along the flow path, the isotopic composition of the F2 and F3 sediment Hg pools, as well as EFPC biofilm and suspended particulates,[6] shifted toward higher δ^{202}Hg and lower Δ^{199}Hg values (Figure 5, Figure 7). These similarities suggest that the F2 and F3 sediment Hg pools were predominantly derived from biofilm and/or suspended particulates. As suggested by Demers *et al.*,[6] shifts in isotopic composition of the biofilm and suspended particulates may have resulted from photochemical and microbial Hg reduction processes, which could also explain the transient increases in Δ^{199}Hg values of the surface water dissolved phase along the flow path. We also provide an alternative explanation, in which the shift in isotopic composition of biofilm and suspended particulates along the flow path is simply driven by mixing with fine-grained streambed sediment, though photochemical reduction in the particulate phase would still be required to explain the isotopic patterns in the dissolved phase. Additionally, it appears that weakly-bound sediment Hg is transferred into the biofilm and suspended particulates, which may subsequently contribute to and shift the isotopic composition of the organically-bound sediment Hg pools as the biofilm and suspended particulates become incorporated into the streambed sediment along the flow path. Biofilm is known to be a site for enhanced Hg methylation within EFPC[80] and other streams, thus legacy Hg that is transferred into biofilm may be more available for methylation and subsequent bioaccumulation in the food web. Additionally, Zhang *et al.*[91] recently showed that in a laboratory setting, up to 7% of EFPC sediment-bound Hg was available for microbial methylation without first being dissolved. For most of our sediment samples, this percentage is greater than the F1, F2, and F3 Hg fractions combined (Table S6). Further studies will be required to determine which of the sediment Hg pools would be preferentially methylated, and to assess the potential transfer of legacy Hg from sediment into biofilm, its transformation into methylmercury, and its incorporation into the food web.

Our coupling of sequential extractions and Hg isotope analysis has highlighted knowledge gaps in our understanding of the mechanisms underlying the biogeochemical cycling of Hg within contaminated stream ecosystems and their associated isotope fractionation patterns. In particular, sequential extraction results point toward a mechanism of dissolution of recalcitrant legacy Hg that does not induce significant isotope fractionation. While the observed isotopic fractionation, or lack-thereof, in our study (and others) suggests that dissolution of recalcitrant Hg may indeed be occurring within the environment, isotope fractionation during dissolution of HgS by most reactions (e.g., dissolution by dissolved organic matter, high levels of dissolved

oxygen, or sulfur-oxidizing bacteria) has not been experimentally evaluated. Moreover, the processes that control the transfer of Hg from weakly-bound fractions to organically-bound fractions need to be identified and their isotopic systematics described. Also, for contaminated ecosystems that are known to contain both Hg(0) and Hg(II), it is worth considering the degree to which equilibrium isotope effects may be ubiquitously over-printing fractionation signatures from kinetic reaction mechanisms, as may be indicated by previous experimental results involving isotope exchange following dark abiotic oxidation.[69] To better constrain and interpret field observations of Hg isotopic composition, it will be necessary to continue to experimentally assess the isotope fractionation associated with environmentally-relevant processes and to expand upon our catalogue of process-specific diagnostic Hg fractionation patterns (i.e., characteristic isotope ratios and slopes).

Overall, Hg isotopic analysis of EFPC surface water, hyporheic pore water, biofilm, suspended particulates, and streambed sediment sequential extractions has provided evidence that sediment-bound legacy Hg may be remobilized within contaminated streams. Together with dissolved Hg flux measurements, this information further suggests that recalcitrant legacy Hg has the potential to be a long-term source of dissolved Hg to stream water, as the large reservoirs of recalcitrant Hg may continue to release small, but meaningful, amounts of Hg. Moreover, our sequential extraction data suggest that remobilized recalcitrant legacy Hg may be incorporated into streambed biofilm, a basal resource of aquatic food webs. Thus, along with reducing dissolved Hg inputs from upstream point sources, remediation efforts focused on the streambed sediment-bound Hg would also likely decrease surface water dissolved Hg concentrations and may also decrease THg and methylmercury concentrations in aquatic organisms.

Conflicts of Interest

There are no conflicts to declare.

Acknowledgements

We thank Todd Olsen for assistance in collecting the biofilm samples that were used for the organic carbon analysis. This manuscript was improved substantially thanks to the thoughtful comments of Jan Wiederhold and two anonymous reviewers. This research was supported by the U.S. Department of Energy (DOE), Office of Science, Biological and Environmental Research

(BER), Subsurface Biogeochemical Research (SBR) program under Award No. DE-SC0016489 and is also a product of the Mercury Science Focus Area (SFA) at Oak Ridge National Laboratory (ORNL). ORNL is managed by UT-Battelle, LLC for the DOE under Contract No. DE-AC05-00OR22725.

REFERENCES

1. A. M. Scheuhammer, M. W. Meyer, M. B. Sandheinrich and M. W. Murray, Effects of environmental methylmercury on the health of wild birds, mammals, and fish, *Ambio*, 2007, **36**, 12-18.
2. Y.-S. Hong, Y.-M. Kim and K.-E. Lee, Methylmercury exposure and health effects, *J. Prev. Med. Public Health*, 2012, **45**, 353-363.
3. UNEP, *Global Mercury Assessment 2013: Sources, Emissions, Releases and Environmental Transport*, UNEP Chemicals Branch, Geneva, Switzerland, 2013.
4. R. R. Turner and G. R. Southworth, Mercury-contaminated industrial and mining sites in North America: an overview with selected case studies, in *Mercury Contaminated Sites–Characterization, Risk Assessment and Remediation*, eds. R. Ebinghaus, R. R. Turner, L. D. de Lacerda, O. Vasiliev and W. Salomons, Springer-Verlag Berlin Heidelberg, 1999, pp. 89-112.
5. K.-Y. Choe, G. A. Gill, R. D. Lehman, S. Han, W. A. Heim and K. H. Coale, Sediment-water exchange of total mercury and monomethyl mercury in the San Francisco Bay-Delta, *Limnol. Oceanogr.*, 2004, **49**, 1512-1527.
6. J. D. Demers, J. D. Blum, S. C. Brooks, P. M. Donovan, A. L. Riscassi, C. L. Miller, W. Zheng and B. Gu, Hg isotopes reveal in-stream processing and legacy inputs in East Fork Poplar Creek, Oak Ridge, Tennessee, USA, *Environ. Sci.: Processes Impacts*, 2018, **20**, 686-707.
7. J. W. M. Rudd, R. A. Bodaly, N. S. Fisher, C. A. Kelly, D. Kopec and C. Whipple, Fifty years after its discharge, methylation of legacy mercury trapped in the Penobscot Estuary sustains high mercury in biota, *Sci. Total Environ.*, 2018, **642**, 1340-1352.
8. S. E. Janssen, M. T. Tate, D. P. Krabbenhoft, J. F. DeWild, J. M. Ogorek, C. L. Babiarz, A. Sowers and P. L. Tuttle, The influence of legacy contamination on the transport and bioaccumulation of mercury within the Mobile River Basin, *J. Hazard. Mater.*, 2020, **404 A**, 124097.
9. E. R. Rothschild, R. R. Turner, S. H. Stow, M. A. Bogle, L. K. Hyder, O. M. Sealand and H. J. Wyrick, *Investigation of Subsurface Mercury at the Oak Ridge Y-12 Plant*, ORNL/TM-9092, Oak Ridge National Laboratory, Oak Ridge, TN, 1984.
10. S. C. Brooks and G. R. Southworth, History of mercury use and environmental contamination at the Oak Ridge Y-12 Plant, *Environ. Pollut.*, 2011, **159**, 219-228.
11. WRRP and UCOR, *2019 Remediation Effectiveness Report for the U.S. Department of Energy Oak Ridge Site, Oak Ridge, Tennessee: Data and Evaluations*, DOE/OR/01-2787&D1, prepared by the Water Resources Restoration Program and UCOR, an AECOM-led partnership with Jacobs, 2019.
12. WRRP and UCOR, *2016 Remediation Effectiveness Report for the U.S. Department of Energy Oak Ridge Reservation, Oak Ridge, Tennessee: Data and Evaluations*,

DOE/OR/01-2707&D1, prepared by the Water Resources Restoration Program and URS | CH2M Oak Ridge LLC, 2016.

13. M. J. Peterson, S. C. Brooks, T. J. Mathews, M. A. Mayes, A. Johs, R. McManamay, D. B. Watson, K. Muller, L. Goñez-Rodríguez, C. DeRolph and S. Nair, *Mercury Remediation Technology Development for Lower East Fork Poplar Creek–FY 2018 Update*, ORNL/SPR-2018/912, Oak Ridge National Laboratory, Oak Ridge, TN, 2018.
14. S. Brooks, V. Eller, J. Dickson, J. Earles, K. Lowe, T. Mehlhorn, T. Olsen, C. DeRolph, D. Watson, D. Phillips and M. Peterson, *Mercury Content of Sediments in East Fork Poplar Creek: Current Assessment and Past Trends*, ORNL/TM-2016/578, Oak Ridge National Laboratory, Oak Ridge, TN, 2017.
15. D. Watson, S. Brooks, T. Mathews, M. Bevelhimer, C. DeRolph, C. Brandt, M. Peterson and R. Ketelle, *Evaluation of Lower East Fork Poplar Creek Mercury Sources*, ORNL/TM-2016/134, Oak Ridge National Laboratory, Oak Ridge, TN, 2016.
16. D. Watson, M. Bevelhimer, C. Brandt, C. DeRolph, S. Brooks, M. Mayes, T. Olsen, J. Dickson, M. Peterson and R. Ketelle, *Evaluation of Lower East Fork Poplar Creek Mercury Sources–Model Update*, ORNL/SR-2016/503, Oak Ridge National Laboratory, Oak Ridge, TN, 2016.
17. J. O. Dickson, M. A. Mayes, S. C. Brooks, T. L. Mehlhorn, K. A. Lowe, J. K. Earles, L. Goñez-Rodríguez, D. B. Watson and M. J. Peterson, Source relationships between streambank soils and streambed sediments in a mercury-contaminated stream, *J. Soils Sediments*, 2019, **19**, 2007-2019.
18. M. J. Peterson, M. Mayes, S. Brooks, T. Mathews, A. Johs, L. Goñez-Rodríguez, C. DeRolph, E. Pierce, D. Watson, K. Muller, T. Olsen, K. Lowe, R. McManamay, J. Smith, J. Morris and M. Jones, *Mercury Remediation Technology Development for Lower East Fork Poplar Creek–2017 Progress Report*, ORNL/TM-2017/480, Oak Ridge National Laboratory, Oak Ridge, TN, 2018.
19. M. O. Barnett, L. A. Harris, R. R. Turner, R. J. Stevenson, T. J. Henson, R. C. Melton and D. P. Hoffman, Formation of mercuric sulfide in soil, *Environ. Sci. Technol.*, 1997, **31**, 3037-3043.
20. P. L. Brezonik and W. A. Arnold, Solubility: reactions of solid phases with water, in *Water Chemistry: An Introduction to the Chemistry of Natural and Engineered Aquatic Systems*, Oxford University Press, Inc., Oxford, New York, 2011, pp. 364-405.
21. Y. Chen, Y. Yin, J. Shi, G. Liu, L. Hu, J.-F. Liu, Y. Cai and G. Jiang, Analytical methods, formation, and dissolution of cinnabar and its impact on environmental cycle of mercury, *Crit. Rev. Environ. Sci. Technol.*, 2017, **47**, 2415-2447.
22. M. Ravichandran, G. R. Aiken, M. M. Reddy and J. N. Ryan, Enhanced dissolution of cinnabar (mercuric sulfide) by dissolved organic matter isolated from the Florida Everglades, *Environ. Sci. Technol.*, 1998, **32**, 3305-3311.
23. J. S. Waples, K. L. Nagy, G. R. Aiken and J. N. Ryan, Dissolution of cinnabar (HgS) in the presence of natural organic matter, *Geochim. Cosmochim. Acta*, 2005, **69**, 1575-1588.
24. A. I. Vázquez-Rodríguez, C. M. Hansel, T. Zhang, C. H. Lamborg, C. M. Santelli, S. M. Webb and S. C. Brooks, Microbial- and thiosulfate-mediated dissolution of mercury sulfide minerals and transformation to gaseous mercury, *Front. Microbiol.*, 2015, **6**, 1-11.
25. Y. H. Hsieh, S. Tokunaga and C. P. Huang, Some chemical reactions at the HgS(s)-water interface as affected by photoirradiation, *Colloids Surf.*, 1991, **53**, 257-274.

26. M. O. Barnett, R. R. Turner and P. C. Singer, Oxidative dissolution of metacinnabar (β-HgS) by dissolved oxygen, *Appl. Geochem.*, 2001, **16**, 1499-1512.
27. E. A. Holley, A. J. McQuillan, D. Craw, J. P. Kim and S. G. Sander, Mercury mobilization by oxidative dissolution of cinnabar (α-HgS) and metacinnabar (β-HgS), *Chem. Geol.*, 2007, **240**, 313-325.
28. N. Issaro, C. Abi-Ghanem and A. Bermond, Fractionation studies of mercury in soils and sediments: A review of the chemical reagents used for mercury extraction, *Anal. Chim. Acta*, 2009, **631**, 1-12.
29. A. Riscassi, C. Miller and S. Brooks, Seasonal and flow-driven dynamics of particulate and dissolved mercury and methylmercury in a stream impacted by an industrial mercury source, *Environ. Toxicol. Chem.*, 2016, **35**, 1386-1400.
30. J. D. Blum, L. S. Sherman and M. W. Johnson, Mercury isotopes in earth and environmental sciences, *Annu. Rev. Earth Planet. Sci.*, 2014, **42**, 249-269.
31. G. Bartov, Ph.D. Thesis, University of Illinois at Urbana-Champaign, 2014.
32. P. M. Donovan, J. D. Blum, J. D. Demers, B. Gu, S. C. Brooks and J. Peryam, Identification of multiple mercury sources to stream sediments near Oak Ridge, TN, USA, *Environ. Sci. Technol.*, 2014, **48**, 3666-3674.
33. S. J. Stetson, J. E. Gray, R. B. Wanty and D. L. Macalady, Isotopic variability of mercury in ore, mine-waste calcine, and leachates of mine-waste calcine from areas mined for mercury, *Environ. Sci. Technol.*, 2009, **43**, 7331-7336.
34. J. G. Wiederhold, R. S. Smith, H. Siebner, A. D. Jew, G. E. Brown Jr., B. Bourdon and R. Kretzschmar, Mercury isotope signatures as tracers for Hg cycling at the New Idria Hg Mine, *Environ. Sci. Technol.*, 2013, **47**, 6137-6145.
35. R. Yin, X. Feng, J. Wang, Z. Bao, B. Yu and J. Chen, Mercury isotope variations between bioavailable mercury fractions and total mercury in mercury contaminated soil in Wanshan Mercury Mine, SW China, *Chem. Geol.*, 2013, **336**, 80-86.
36. J. G. Wiederhold, U. Skyllberg, A. Drott, M. Jiskra, S. Jonsson, E. Björn, B. Bourdon and R. Kretzschmar, Mercury isotope signatures in contaminated sediments as a tracer for local industrial pollution sources, *Environ. Sci. Technol.*, 2015, **49**, 177-185.
37. F. M. Brocza, H. Biester, J.-H. Richard, S. M. Kraemer and J. G. Wiederhold, Mercury isotope fractionation in the subsurface of a Hg(II) chloride-contaminated industrial legacy site, *Environ. Sci. Technol.*, 2019, **53**, 7296-7305.
38. A. R. C. Grigg, R. Kretzschmar, R. S. Gilli and J. G. Wiederhold, Mercury isotope signatures of digests and sequential extracts from industrially contaminated soils and sediments, *Sci. Total Environ.*, 2018, **636**, 1344-1354.
39. S. Huang, Y. Zhao, S. Lv, W. Wang, W. Wang, Y. Zhang, Y. Huo, X. Sun and Y. Chen, Distribution of mercury isotope signatures in Yundang Lagoon, Xiamen, China, after long-term interventions, *Chemosphere*, 2021, **272**, 129716.
40. M. J. Peterson, S. C. Brooks, T. J. Mathews, M. Mayes, A. Johs, D. B. Watson, M. D. Poteat, J. G. Smith, T. Mehlhorn, B. Lester, J. Morris, K. Lowe, J. O. Dickson, V. Eller and C. R. DeRolph, *Mercury Remediation Technology Development for Lower East Fork Poplar Creek–FY 2015 Progress Report*, ORNL/TM-2016/48, Oak Ridge National Laboratory, Oak Ridge, TN, 2016.
41. J. D. Demers, J. D. Blum and D. R. Zak, Mercury isotopes in a forested ecosystem: Implications for air-surface exchange dynamics and the global mercury cycle, *Global Biogeochem. Cycles*, 2013, **27**, 222-238.

42. U. S. EPA, *Method 1631, Revision E: Mercury in Water by Oxidation, Purge and Trap, and Cold Vapor Atomic Fluorescence Spectrometry*, EPA-821-R-02-019, U.S. Environmental Protection Agency, Office of Water, Washington, D.C., 2002.
43. N. S. Bloom, E. Preus, J. Katon and M. Hiltner, Selective extractions to assess the biogeochemically relevant fractionation of inorganic mercury in sediments and soils, *Anal. Chim. Acta*, 2003, **479**, 233-248.
44. G. Liu, J. Cabrera, M. Allen and Y. Cai, Mercury characterization in a soil sample collected nearby the DOE Oak Ridge Reservation utilizing sequential extraction and thermal desorption method, *Sci. Total Environ.*, 2006, **369**, 384-392.
45. G. Southworth, M. Greeley, M. Peterson, K. Lowe and R. Ketelle, *Sources of Mercury to East Fork Poplar Creek Downstream from the Y-12 National Security Complex: Inventories and Export Rates*, ORNL/TM-2009/231, Oak Ridge National Laboratory, Oak Ridge, TN, 2010.
46. C. L. Miller, D. B. Watson, B. P. Lester, K. A. Lowe, E. M. Pierce and L. Liang, Characterization of soils from an industrial complex contaminated with elemental mercury, *Environ. Res.*, 2013, **125**, 20-29.
47. G. E. M. Hall, P. Pelchat and J. B. Percival, The design and application of sequential extractions for mercury, Part 1. Optimization of HNO3 extraction for all non-sulphide forms of Hg, *Geochem.: Explor. Environ., Anal.*, 2005, **5**, 107-113.
48. G. E. M. Hall and P. Pelchat, The design and application of sequential extractions for mercury, Part 2. Resorption of mercury onto the sample during leaching, *Geochem.: Explor. Environ., Anal.*, 2005, **5**, 115-121.
49. M. L. Olson, L. B. Cleckner, J. P. Hurley, D. P. Krabbenhoft and T. W. Heelan, Resolution of matrix effects on analysis of total and methyl mercury in aqueous samples from the Florida Everglades, *Fresenius J. Anal. Chem.*, 1997, **358**, 392-396.
50. J. D. Demers, J. B. Yavitt, C. T. Driscoll and M. R. Montesdeoca, Legacy mercury and stoichiometry with C, N, and S in soil, pore water, and stream water across the upland-wetland interface: The influence of hydrogeologic setting, *J. Geophys. Res.: Biogeosci.*, 2013, **118**, 825-841.
51. N. W. Revis, T. R. Osborne, D. Sedgley and A. King, Quantitative method for determining the concentration of mercury(II) sulphide in soils and sediments, *Analyst*, 1989, **114**, 823-825.
52. C. S. Kim, N. S. Bloom, J. J. Rytuba and G. E. Brown Jr., Mercury speciation by X-ray absorption fine structure spectroscopy and sequential chemical extractions: A comparison of speciation methods, *Environ. Sci. Technol.*, 2003, **37**, 5102-5108.
53. R. P. Eganhouse, D. R. Young and J. N. Johnson, Geochemistry of mercury in Palos Verdes sediments, *Environ. Sci. Technol.*, 1978, **12**, 1151-1157.
54. D. S. Lauretta, B. Klaue, J. D. Blum and P. R. Buseck, Mercury abundances and isotopic compositions in the Murchison (CM) and Allende (CV) carbonaceous chondrites, *Geochim. Cosmochim. Acta*, 2001, **65**, 2807-2818.
55. J. D. Blum and B. A. Bergquist, Reporting of variations in the natural isotopic composition of mercury, *Anal. Bioanal. Chem.*, 2007, **388**, 353-359.
56. J. D. Blum and M. W. Johnson, Recent developments in mercury stable isotope analysis, *Rev. Mineral. Geochem.*, 2017, **82**, 733-757.

57. Q. Wang, Y. Li and Y. Wang, Optimizing the weight loss-on-ignition methodology to quantify organic and carbonate carbon of sediments from diverse sources, *Environ. Monit. Assess.*, 2011, **174**, 241-257.
58. D. W. Pribyl, A critical review of the conventional SOC to SOM conversion factor, *Geoderma*, 2010, **156**, 75-83.
59. D. York, Least-squares fitting of a straight line, *Can. J. Phys.*, 1966, **44**, 1079-1086.
60. P. Vermeesch, IsoplotR: A free and open toolbox for geochronology, *Geosci. Front.*, 2018, **9**, 1479-1493.
61. J. G. Wiederhold, S. M. Kraemer, N. Teutsch, P. M. Borer, A. N. Halliday and R. Kretzschmar, Iron isotope fractionation during proton-promoted, ligand-controlled, and reductive dissolution of goethite, *Environ. Sci. Technol.*, 2006, **40**, 3787-3793.
62. L. E. Gratz, G. J. Keeler, J. D. Blum and L. S. Sherman, Isotopic composition and fractionation of mercury in Great Lakes precipitation and ambient air, *Environ. Sci. Technol.*, 2010, **44**, 7764-7770.
63. J. Chen, H. Hintelmann, X. Feng and B. Dimock, Unusual fractionation of both odd and even mercury isotopes in precipitation from Peterborough, ON, Canada, *Geochim. Cosmochim. Acta*, 2012, **90**, 33-46.
64. E. A. Schauble, Role of nuclear volume in driving equilibrium stable isotope fractionation of mercury, thallium, and other very heavy elements, *Geochim. Cosmochim. Acta*, 2007, **71**, 2170-2189.
65. J. G. Wiederhold, C. J. Cramer, K. Daniel, I. Infante, B. Bourdon and R. Kretzschmar, Equilibrium mercury isotope fractionation between dissolved Hg(II) species and thiol-bound Hg, *Environ. Sci. Technol.*, 2010, **44**, 4191-4197.
66. N. Estrade, J. Carignan, J. E. Sonke and O. F. X. Donard, Mercury isotope fractionation during liquid-vapor evaporation experiments, *Geochim. Cosmochim. Acta*, 2009, **73**, 2693-2711.
67. S. Ghosh, E. A. Schauble, G. L. Couloume, J. D. Blum and B. A. Bergquist, Estimation of nuclear volume dependent fractionation of mercury isotopes in equilibrium liquid-vapor evaporation experiments, *Chem. Geol.*, 2013, **336**, 5-12.
68. M. Jiskra, J. G. Wiederhold, B. Bourdon and R. Kretzschmar, Solution speciation controls mercury isotope fractionation of Hg(II) sorption to goethite, *Environ. Sci. Technol.*, 2012, **46**, 6654-6662.
69. W. Zheng, J. D. Demers, X. Lu, B. A. Bergquist, A. D. Anbar, J. D. Blum and B. Gu, Mercury stable isotope fractionation during abiotic dark oxidation in the presence of thiols and natural organic matter, *Environ. Sci. Technol.*, 2019, **53**, 1853-1862.
70. S. Yang and Y. Liu, Nuclear volume effects in equilibrium stable isotope fractionations of mercury, thallium and lead, *Sci. Rep.*, 2015, **5**, 12626.
71. A. L. Buchachenko, Mercury isotope effects in the environmental chemistry and biochemistry of mercury-containing compounds, *Russ. Chem. Rev.*, 2009, **78**, 319-328.
72. W. Zheng and H. Hintelmann, Mercury isotope fractionation during photoreduction in natural water is controlled by its Hg/DOC ratio, *Geochim. Cosmochim. Acta*, 2009, **73**, 6704-6715.
73. W. Zheng and H. Hintelmann, Nuclear field shift effect in isotope fractionation of mercury during abiotic reduction in the absence of light, *J. Phys. Chem. A*, 2010, **114**, 4238-4245.

74. R. Sun, D. G. Streets, H. M. Horowitz, H. M. Amos, G. Liu, V. Perrot, J.-P. Toutain, H. Hintelmann, E. M. Sunderland and J. E. Sonke, Historical (1850-2010) mercury stable isotope inventory from anthropogenic sources to the atmosphere, *Elem.: Sci. Anth.*, 2016, **4**, 1-15.
75. D. Foucher, H. Hintelmann, T. A. Al and K. T. MacQuarrie, Mercury isotope fractionation in waters and sediments of the Murray Brook mine watershed (New Brunswick, Canada): Tracing mercury contamination and transformation, *Chem. Geol.*, 2013, **336**, 87-95.
76. R. S. Smith, J. G. Wiederhold and R. Kretzschmar, Mercury isotope fractionation during precipitation of metacinnabar (β-HgS) and montroydite (HgO), *Environ. Sci. Technol.*, 2015, **49**, 4325-4334.
77. E. J. Schnabel, S. Butler, C. Ahlem, J. Papazian, C. Pedersen, W. Porter, J. Sharrah, P. M. Smith, C. C. Wisdom and G. M. Carlton, *Mercury Concentrations and Loads from the Sacramento River and from Cache Creek to the Sacramento-San Joaquin Delta Estuary*, California Regional Water Quality Control Board, Central Valley Region, 1998.
78. J. J. Rytuba, Mercury mine drainage and processes that control its environmental impact, *Sci. Total Environ.*, 2000, **260**, 57-71.
79. P. M. Donovan, J. D. Blum, M. B. Singer, M. Marvin-DiPasquale and M. T. K. Tsui, Methylmercury degradation and exposure pathways in streams and wetlands impacted by historical mining, *Sci. Total Environ.*, 2016, **568**, 1192-1203.
80. T. A. Olsen, C. C. Brandt and S. C. Brooks, Periphyton biofilms influence net methylmercury production in an industrially contaminated system, *Environ. Sci. Technol.*, 2016, **50**, 10843-10850.
81. P. Jiang, Y. Li, G. Liu, G. Yang, L. Lagos, Y. Yin, B. Gu, G. Jiang and Y. Cai, Evaluating the role of re-adsorption of dissolved Hg2+ during cinnabar dissolution using isotope tracer technique, *J. Hazard. Mater.*, 2016, **317**, 466-475.
82. Y. Yin, H. E. Allen, C. P. Huang, D. L. Sparks and P. F. Sanders, Kinetics of mercury(II) adsorption and desorption on soil, *Environ. Sci. Technol.*, 1997, **31**, 496-503.
83. P. Pelcová, J. Margetínová, T. Vaculovič, J. Komárek and V. Kubáň, Adsorption of mercury species on river sediments – effects of selected abiotic parameters, *Cent. Eur. J. Chem.*, 2010, **8**, 116-125.
84. S. M. Hasany, M. M. Saeed and M. Ahmed, Retention of Hg(II) by solid mercury sulfide from acidic solution, *Sep. Sci. Technol.*, 1999, **34**, 487-499.
85. L. Zhang, X. Liang, Q. Wang, Y. Zhang, X. Yin, X. Lu, E. M. Pierce and B. Gu, Isotope exchange between mercuric [Hg(II)] chloride and Hg(II) bound to minerals and thiolate ligands: Implications for enriched isotope tracer studies, *Geochim. Cosmochim. Acta*, 2021, **292**, 468-481.
86. J. G. Wiederhold, Metal stable isotope signatures as tracers in environmental geochemistry, *Environ. Sci. Technol.*, 2015, **49**, 2606-2624.
87. B. Gu, B. Mishra, C. Miller, W. Wang, B. Lai, S. C. Brooks, K. M. Kemner and L. Liang, X-ray fluorescence mapping of mercury on suspended mineral particles and diatoms in a contaminated freshwater system, *Biogeosciences*, 2014, **11**, 5259-5267.
88. J. D. Newbold, J. W. Elwood, R. V. O'Neill and W. Van Winkle, Measuring nutrient spiralling in streams, *Can. J. Fish. Aquat. Sci.*, 1981, **38**, 860-863.

89. W. Zheng and H. Hintelmann, Isotope fractionation of mercury during its photochemical reduction by low-molecular-weight organic compounds, *J. Phys. Chem. A*, 2010, **114**, 4246-4253.
90. B. A. Bergquist and J. D. Blum, Mass-dependent and -independent fractionation of Hg isotopes by photoreduction in aquatic systems, *Science*, 2007, **318**, 417-420.
91. L. Zhang, S. Wu, L. Zhao, X. Lu, E. M. Pierce and B. Gu, Mercury sorption and desorption on organo-mineral particulates as a source for microbial methylation, *Environ. Sci. Technol.*, 2019, **53**, 2426-2433.

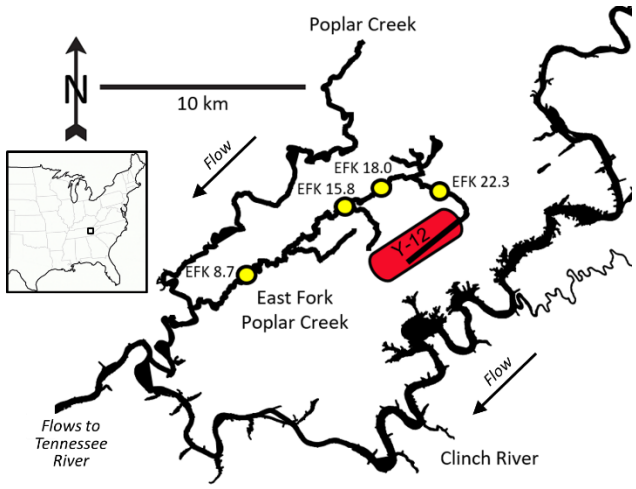

Figure 1: Map of East Fork Poplar Creek in Oak Ridge, Tennessee, USA, highlighting the Y-12 National Security Complex (red oval) and the four streambed sediment collection sites: EFK 22.3, EFK 18.0, EFK 15.8, and EFK 8.7 (yellow circles).

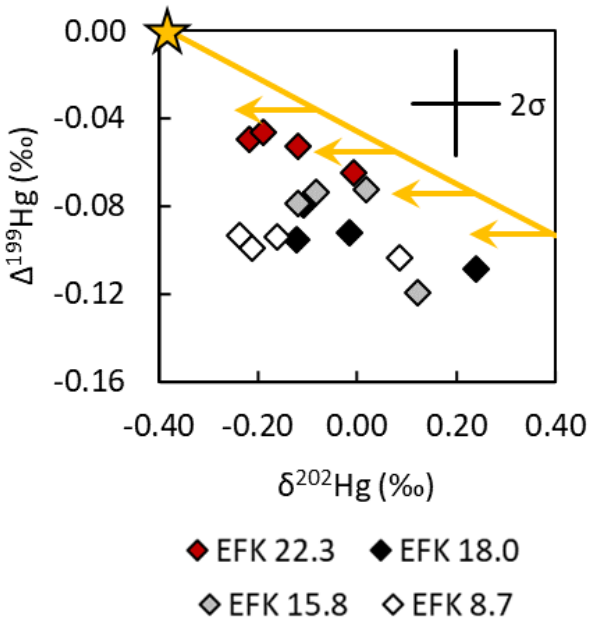

Figure 2: Total Hg isotopic composition of EFPC streambed sediment, measured via combustion. Analytical uncertainty in delta values is shown as the average uncertainty (2SD) across combustion reference material analyses (see Section 2.5). The gold star represents the assumed isotopic composition of metallic Hg(0) historically used at Y-12 (average isotopic composition of -0.38 ± 0.34‰ δ^{202}Hg and near-zero Δ^{199}Hg).[74] The diagonal line represents the equilibrium isotope effect driven by isotope exchange between coexisting Hg(0) and Hg(II) species (Δ^{199}Hg/δ^{202}Hg slope of -0.12 ± 0.01, 1SE).[69] This is followed by precipitation of HgS and other minerals,[75,76] sorption of Hg(II) to mineral surfaces,[68] and/or binding of Hg(II) to thiol ligands within organic matter[65] (horizontal arrows pointing toward lower δ^{202}Hg values for the solid phase).

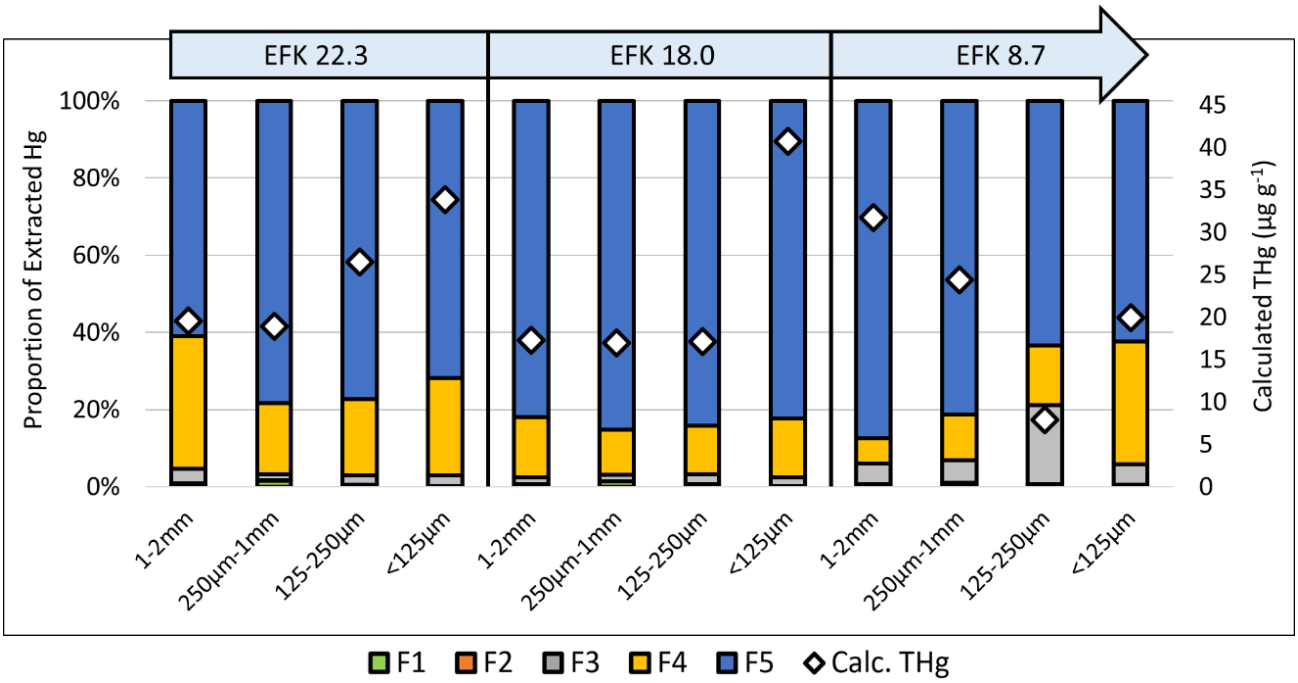

Figure 3: Proportions of Hg fractions extracted from EFPC streambed sediment (bar graph, left axis) and total Hg concentration calculated from the sum of sequential extractions (white diamonds, right axis.) Note that the proportions of F1 and F2 are too small to be visible on the figure.

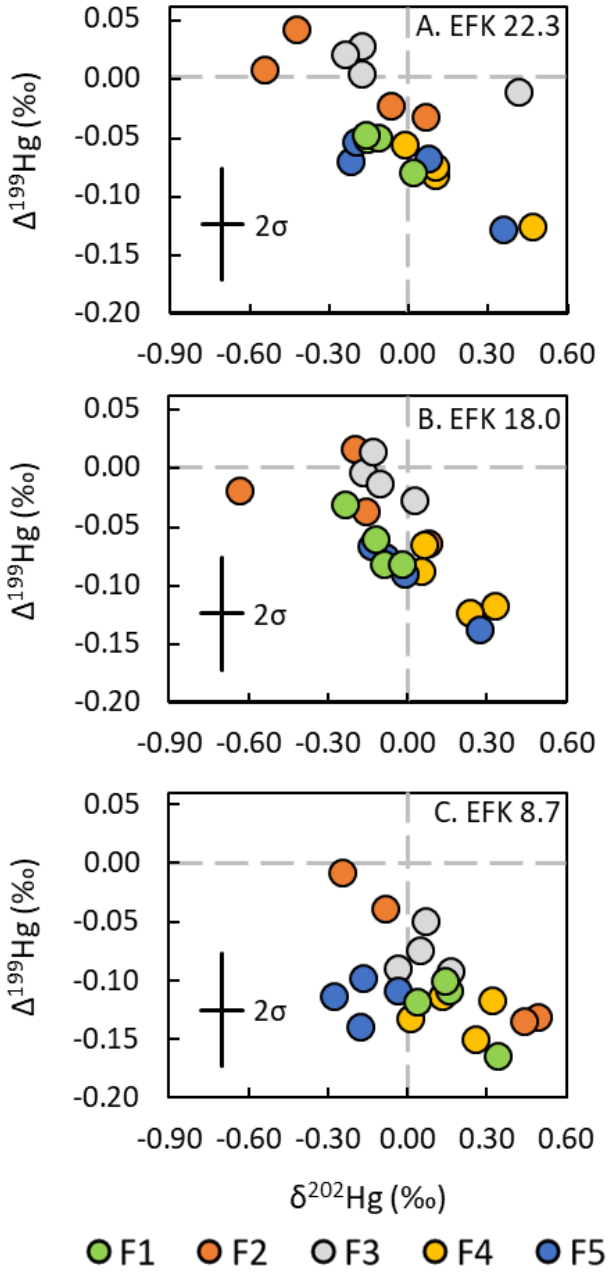

Figure 4: Mercury isotopic composition of sequential extractions of EFPC streambed sediment collected from (A) EFK 22.3, (B) EFK 18.0, and (C) EFK 8.7. Analytical uncertainty in delta values is shown as the average uncertainty (2SD) across all UM-Almadén analyses (see Section 2.5). Symbols of the same color represent different sediment size fractions.

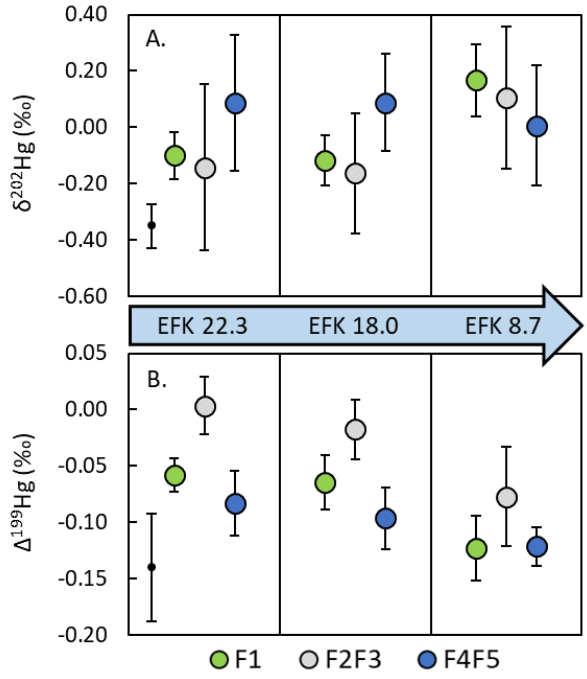

Figure 5: Average Hg isotopic composition of sequential extractions of EFPC streambed sediment. Shown are (A) δ^{202}Hg and (B) Δ^{199}Hg values for F1, F2F3, and F4F5 Hg fractions averaged across all size fractions within each sampling site. Isotopic compositions of the F2F3 and F4F5 Hg fractions were calculated based on the unweighted average of F2 and F3, and of F4 and F5 fractions, respectively. Error bars represent 1SD associated with each average δ^{202}Hg or Δ^{199}Hg value (n=4 for F1 fractions, n=8 for F2F3 and F4F5 fractions). Average and 1SD values match those reported in Table S13. Analytical uncertainty in delta values is shown as the average uncertainty (2SD) across all UM-Almadén analyses (see Section 2.5).

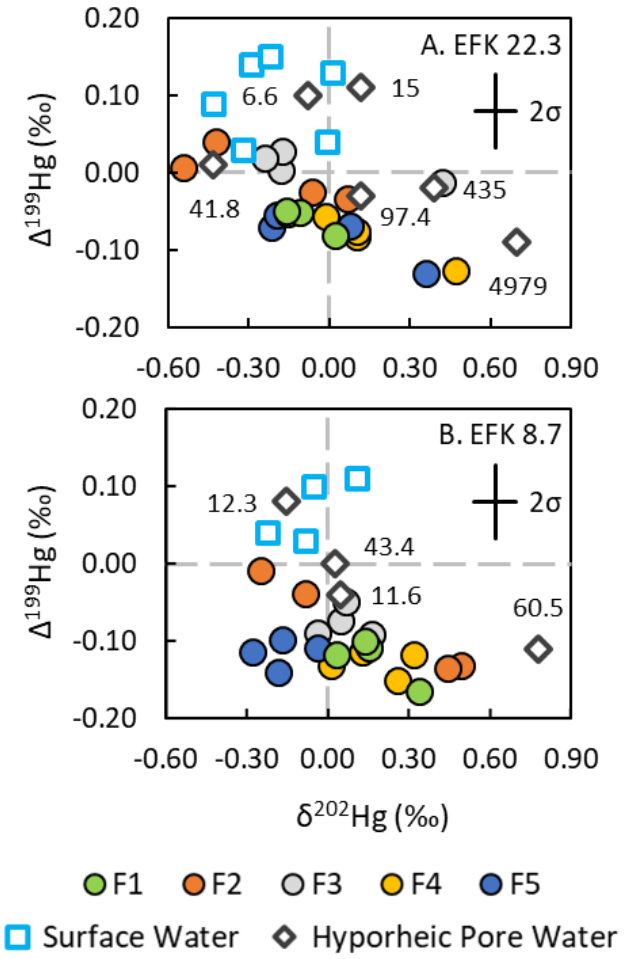

Figure 6: Mercury isotopic composition of sequential extractions of EFPC streambed sediment collected from (A) EFK 22.3 and (B) EFK 8.7, along with surface water and hyporheic pore water dissolved phase collected from (A) EFK 22.3 and (B) EFK 5.0.[6] Dissolved Hg concentrations of the hyporheic pore water samples are shown as numbers on the plots (ng L^{-1}). One EFK 5.0 pore water sample is not shown because it plots off scale at 0.28‰ δ^{202}Hg and 0.37‰ Δ^{199}Hg, and has a dissolved Hg concentration of 6.7 ng L^{-1}. Analytical uncertainty in sequential extraction delta values is shown as the average uncertainty (2SD) across all UM-Almadén analyses (see Section 2.5). Analytical uncertainty for water samples is less than or equal to analytical uncertainty of sequential extraction samples.[6]

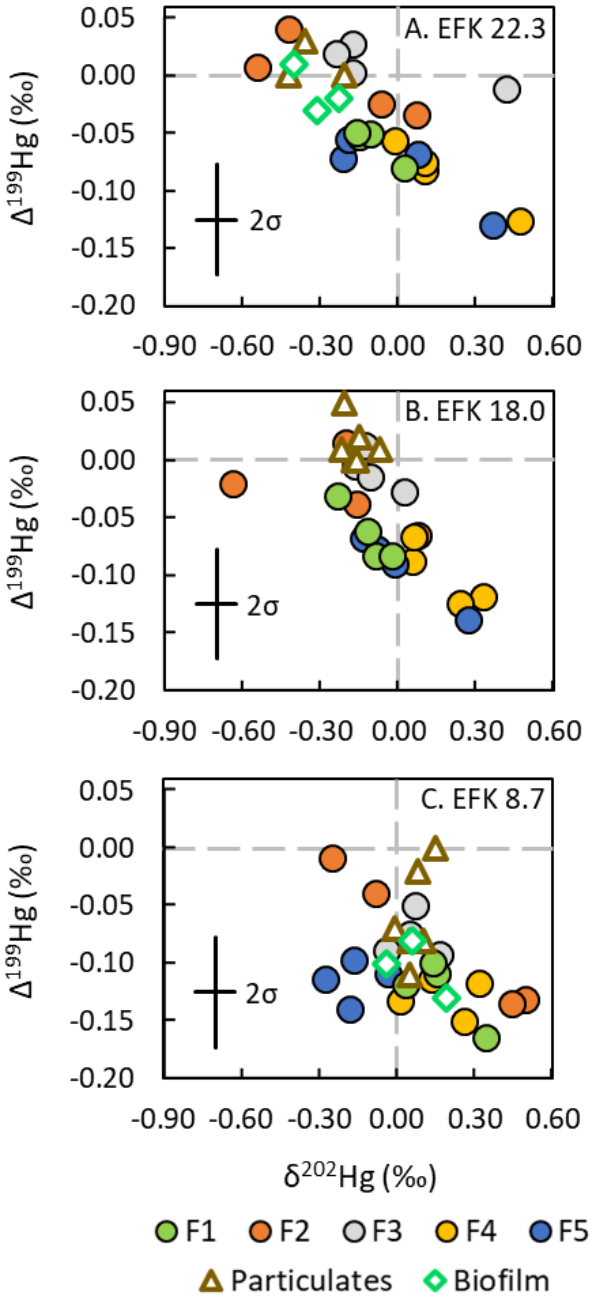

Figure 7: Mercury isotopic composition of sequential extractions of EFPC streambed sediment collected from (A) EFK 22.3, (B) EFK 18.0, and (C) EFK 8.7, along with biofilm collected from (A) EFK 22.3 and (C) EFK 5.0, and suspended particulates collected from (A) EFK 22.3, (B) EFK 18.2, EFK 17.8, (C) EFK 9.8, and EFK 5.0.[6] Analytical uncertainty in sequential extraction delta values is shown as the average uncertainty (2SD) across all UM-Almadén analyses (see Section 2.5). Analytical uncertainty for biofilm and suspended particulate samples is less than or equal to analytical uncertainty of sequential extraction samples.[6]